

Supplementary information for the article:

Future Environmental Impacts of Global Iron and Steel Production

Carina Harpprecht^{a,b,*}, Romain Sacchi^c, Tobias Naegler^a, Mariësse van Sluisveld^d, Vassilis Daioglou^{d,e}, Arnold Tukker^{b,f}, Bernhard Steubing^b

^a German Aerospace Center (DLR), Institute of Networked Energy Systems, Curiestr. 4, 70563 Stuttgart, Germany

^b Leiden University, Institute of Environmental Sciences (CML), P.O.Box 9518, 2300 RA Leiden, The Netherlands

^c Laboratory for Energy Systems Analysis, Centers for Energy and Environmental Sciences and Nuclear Engineering and Sciences, Paul Scherrer Institute, Villigen, Switzerland

^d PBL Netherlands Environmental Assessment Agency, P.O. Box 30314, 2500 GH The Hague, The Netherlands

^e Copernicus Institute of Sustainable Development, Utrecht University, Princetonlaan 8a, 3584 CB, Utrecht, The Netherlands

^f Netherlands Organisation for Applied Scientific Research TNO, Anna van Buerenplein 1, 2595 DA The Hague, The Netherlands

* corresponding author: carina.harpprecht@dlr.de

published in Energy & Environmental Science, 2025

Please note that this supplementary information is complemented by an open-access Zenodo repository:

C. Harpprecht, R. Sacchi, T. Naegler, M. van Sluisveld, V. Daioglou, A. Tukker and B. Steubing, *Code and data for publication: Future Environmental Impacts of Global Iron and Steel Production. v1.0.0, 2025*, <https://doi.org/10.5281/zenodo.14968094>

Abbreviations

Acid.: acidification; **BECCS**: Biomass energy with carbon capture and storage; **BF-BOF**: blast-furnace and basic-oxygen furnace; **BG**: background; **CCS**: carbon capture and storage; **CO**: carbon monoxide; **Ecotox.**: ecotoxicity; **Energy res., non-renew.**: non-renewable energy resources; **ESI**: Electronic supplementary information; **Eutroph., freshwater**: freshwater eutrophication; **Eutroph., marine**: marine eutrophication; **Eutroph, terrestrial**: terrestrial eutrophication; **EW**: electrowinning; **GHG**: greenhouse gas; **GWP**: global warming potential; **H2-DRI**: hydrogen-based direct reduction; **Human tox., carc.**: carcinogenic human toxicity; **Human tox., non-carc.**: non-carcinogenic human toxicity; **IAM**: Integrated Assessment Model; **IMAGE**: Integrated Model to Assess the Global Environment; **ionising rad.**: ionising radiation; **IPCC**: Intergovernmental Panel on Climate Change; **LCA**: life cycle assessment; **LCI**: life cycle inventory; **MEA**: mono-ethanolamine; **NaOH**: sodium hydroxide; **NG-DRI**: natural gas-based direct reduction; **Ozone depl.**: ozone depletion; **PM**: particulate matter; **Photochem. ozone**: photochemical ozone formation; **premise**: PRospective EnvironMental Impact asSEssment; **RCP**: Representative Concentration Pathways; **scrap-EAF**: scrap-based electric arc furnace; **SR-BOF**: smelting reduction and basic-oxygen furnace; **SSP**: shared socio-economic pathways; **TGR-BF-BOF**: top gas recycling blast-furnace and basic-oxygen furnace; **VPSA**: Vacuum Pressure Swing Adsorption.

Table of Contents

Abbreviations.....	1
1 Methods	4
1.1. The IMAGE model.....	4
1.1.1. Overview of IMAGE	4
1.1.2. Parametrization of the steel sector	4
1.1.3. Model regions.....	7
1.1.4. Hydrogen module	9
1.2. Energy and steel scenarios from IMAGE	10
1.2.1. Technology mapping	10
1.2.2. Regional steel production.....	10
1.2.3. Market mixes of steel production	11
1.2.4. Efficiency improvements of iron and steel production.....	15
1.2.5. IMAGE scenario data for energy sectors	20
1.3. Life Cycle Inventories.....	22
1.3.1. Electrowinning.....	26
1.3.2. Carbon capture and storage processes	28
1.3.3. Green H ₂ -DRI.....	29
1.4. Integration of scenario data into ecoinvent.....	30
1.4.1. Premise.....	30
1.4.2. Creation of regional steel markets	30
1.4.3. Creation of a global market group for steel	32
1.4.4. Alloying elements	32
1.4.5. Distinction between primary and secondary steel production.....	34
1.5. Impact assessment methods.....	34
2 Results	36
2.1. Impacts of iron ore pellets and iron sinter production	36
2.2. Specific impacts of steel and electricity markets	37
2.2.1. Steel markets.....	37
2.2.2. Electricity markets	40
2.3. Contribution analysis for specific impacts of global steel production	42
2.3.1. Human toxicity (carcinogenic).....	45
2.3.2. Ionising radiation.....	46
2.3.3. Material resource depletion.....	46
2.3.4. Ozone depletion	47
2.4. Specific impacts under varying background scenarios.....	47
2.5. Normalization and weighting results	52

3	Discussion	55
3.1.	Explorative scenario with a shift to green H ₂ -DRI.....	55
3.2.	Limitations.....	56
3.2.1.	Scenarios from IMAGE.....	56
3.2.2.	Premise.....	59
3.2.3.	LCIs of steel production processes	59
4	References	61

1 Methods

1.1. The IMAGE model

1.1.1. Overview of IMAGE

IMAGE is an Integrated Assessment Model (IAM) of global coverage which models the interaction between the environment and human activities¹. Its goal is to emulate global environmental processes and possible societal development routes induced by innovation and other policy interventions (mostly those related to climate mitigation). As such, it provides insights into contexts where the world continues business as usual and contexts in which environmental policy objectives are attained in varying degrees. Within the range of IAM models, IMAGE is a recursive-dynamic simulation model, placing greater emphasis on material dynamics and technical and biophysical processes, and less so on economic systems.

It is structured in different components, with the Targets IMAge Energy Regional model (TIMER) being one of its major modules. TIMER simulates the dynamics of the energy system for various sectors, such as transport, heavy industry, residential, and services. The steel sector is part of the industry model in TIMER.

The decision module in IMAGE takes into account the costs associated with a production technology, next to other factors, such as CO₂ emissions. Total costs are calculated based on fuel costs, capital and operational expenditures (CAPEX, OPEX), and policy costs, such as carbon pricing. While CAPEX and OPEX are global representations, assuming best-available-technology as reported in empirical literature, fuel prices are endogenously estimated and regionally distinct. For further details on the IMAGE framework, the reader is referred to the related literature¹⁻³.

1.1.2. Parametrization of the steel sector

The general working principle of the steel submodule in IMAGE is described in existing literature¹⁻³ explaining the modelling of steel demand and trade, production routes and end-of-life. Parameters for costs and maximum efficiency improvements are based on van Sluisveld et al. (2021)² (Table S1).

Table S1: Parametrisation of the steel model for costs and efficiency improvements in IMAGE v.3.3 as in van Sluisveld et al. (2021)². CAPEX and OPEX are based on van Ruijven et al. (2016)³.

	Costs		Max. energy efficiency improvement
	CAPEX	OPEX	
Steel production route	(USD\$1995/ton/year)	(USD\$1995/ton/year)	%/year
Standard BF/ BOF	470	88	0.0
Efficient BF/ BOF	602	93	0.0
Standard BF/ BOF + CCS	988	89	0.9
DRI EAF	371	57	0.9
DRI EAF + CCS	746	57	1.1
Efficient BF/ BOF TGR	602	93	0.9
BAT BF/ BOF TGR	831	162	0.0
BAT BF/ BOF TGR+ CCS	1346	162	0.0
SR+BOF	441	88	1.1
SR+BOF+CCS	816	88	1.1
H2 DRI EAF	371	57	0.0
EW/EAF	645	137	0.0
EAF/scrap	-	-	0.9

Updates of the steel model for IMAGE v3.3

For IMAGE v3.3, we updated various parameters with more recent data to better account for the empirical basis for 'best available technologies' and energy requirements of CCS technologies. As a result, the parameters of the specific energy consumption (SEC), the floor value of the SEC, and the CO₂ capture rate were adapted for several technologies. An overview of these updates, including the underlying assumptions and respective data sources, is provided in Table S2 and Figure S1.

Energy use:

- The updates replaced the original parameterisation of a theoretical minimum energy consumption for iron/steel making³ with best-available-technology (BAT) estimates as found in literature.

CO₂ capture rate:

- An energy penalty is added to the use of CCS, allowing the model to account for the additional energy demand of CCS for the steel sector.
- IAMs represent fully integrated production systems for basic materials. Instead of using the capture rate at the level of the specific capture technology, we adopt the average capture rate estimate per ton of steel produced. This then takes into account other flue gases not captured within the production system for iron and steel.

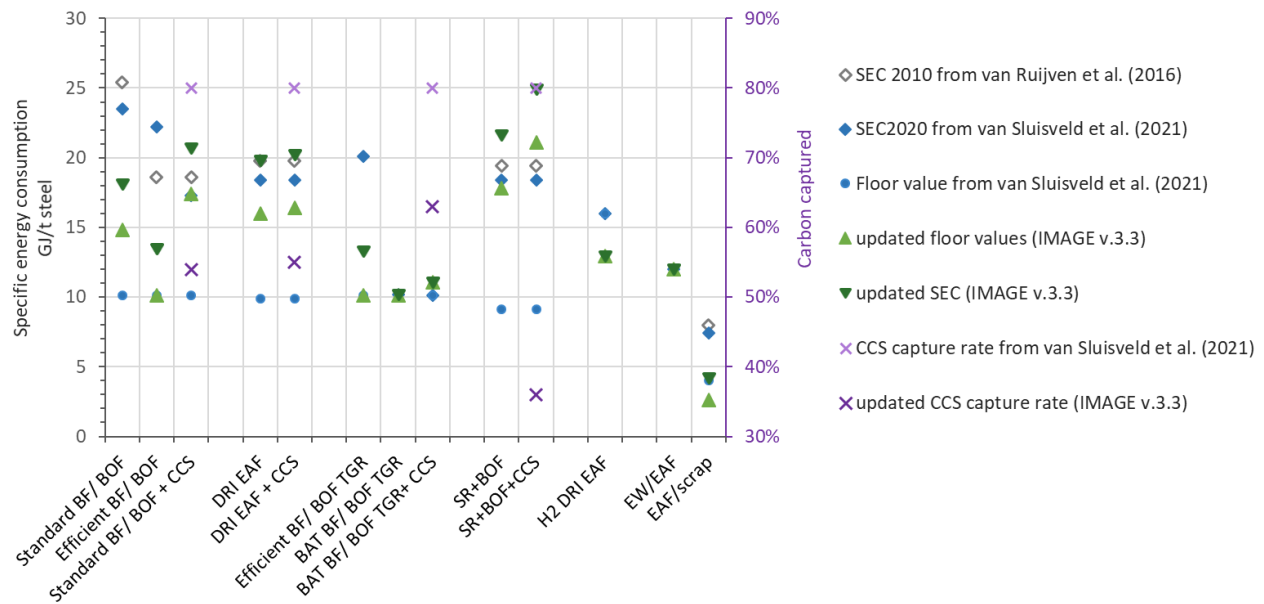


Figure S1: Updates for the parameters of specific energy consumption (SEC, left axis) and carbon capture rates (right axis) for the steel model in IMAGE v3.3 compared to previous IMAGE versions ^{2,3}.

Table S2: Updated parametrisation of the steel model for IMAGE v.3.3 compared to van Sluisveld et al. (2021)².

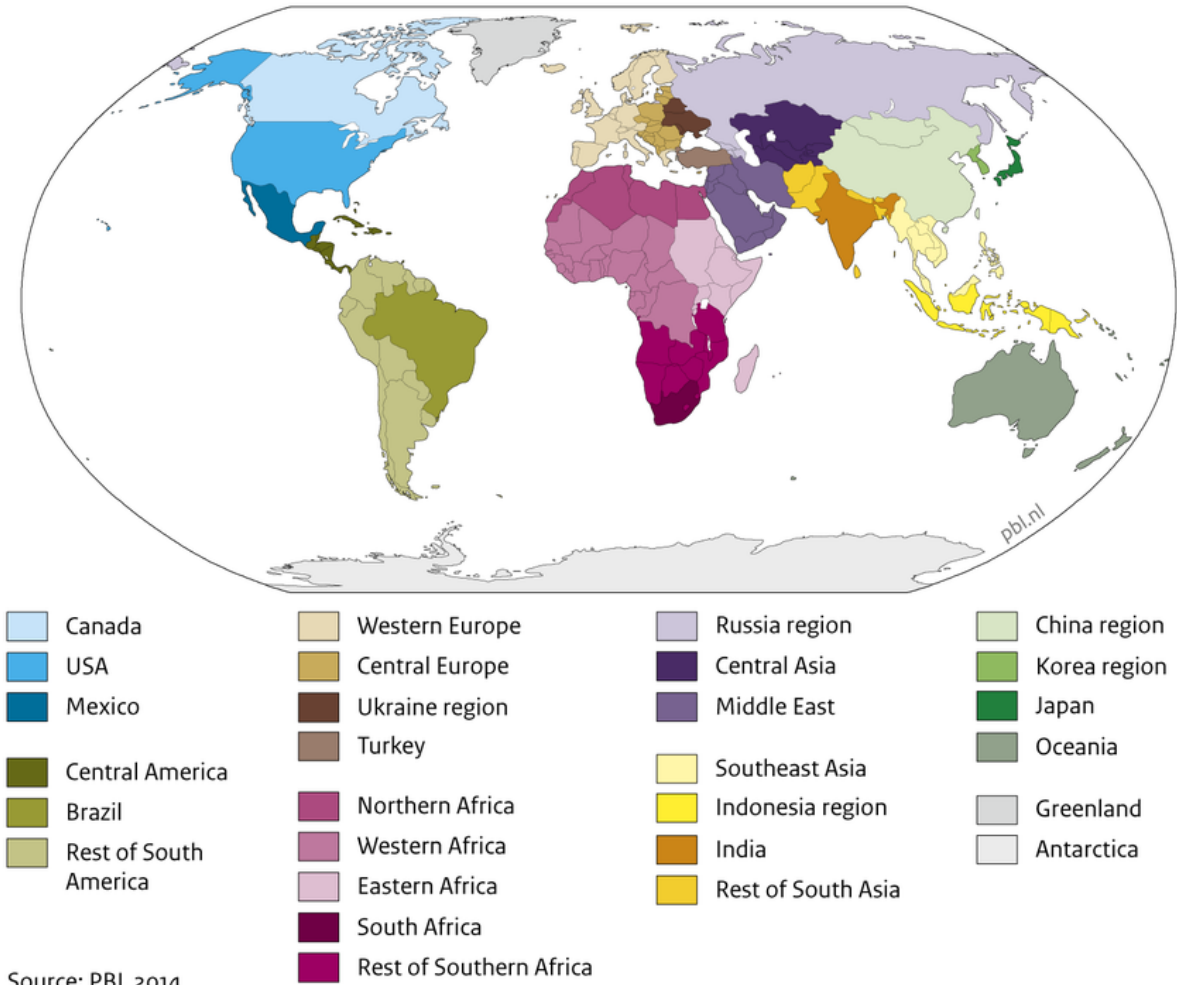
Steel production route in IMAGE	Van Sluisveld et al. 2021			Updated parameters			Data sources for updates		
	SEC ₂₀₂₀	Floor value	CCS capture rate	SEC ₂₀₂₀	Floor value	CCS capture rate	SEC	floor value	CCS capture rate
	GJ/t _{steel}	GJ/t _{steel}	%	GJ/t _{steel}	GJ/t _{steel}	%			
Standard BF-BOF	23.5	10.15	-	18.1	14.8		Arens et al. (2017) ⁴	Worrell et al. (2007) ⁵	-
Efficient BF-BOF	22.2	10.15	-	13.45	10.15		added difference of Worrell et al. (2007) ⁵ and Arens et al. (2017) ⁴ (3.3 GJ / t steel)	unchanged * ¹	-
Standard BF-BOF+CCS	17.3	10.15	80%	20.67	17.37	54%	IEAGHG (2013) ⁶ : added energy for MEA-CCS: 3.37 GJ/tHRC	IEAGHG (2013) ⁶ : added energy for MEA-CCS * ³	IEAGHG (2013) ⁶
DRI EAF	18.4	9.9	-	19.8	16		Arens et al. (2017) ⁴ and Worrell et al. (2007) ⁵	Keys et al. (2019) ⁷	-
DRI EAF+CCS	18.4	9.9	80%	20.19	16.39	55%	Keys et al. (2019) ⁷ : added energy for CCS (0.39 GJ/ t HRC from figure 25, table 8) to SEC of DRI	Keys et al. (2019) ⁷ : added energy for CCS (0.39 GJ/ t HRC from figure 25, table 8) to floor value of DRI	Keys et al. (2019) ⁷
Efficient BF-BOF TGR	20.1	10.15	-	13.3	10.15		Keys et al. (2019) ⁷ (fig. 30, fig. 23)	unchanged	-
BAT BF-BOF TGR	10.2	10.15	-	10.2	10.15		unchanged	unchanged	-
BAT BF-BOF TGR+CCS	10.15	10.15	80%	11.06	11.06	63%	Quader et al. (2016) ⁸ and Keys et al. (2019) ⁷ : added the energy for CCS of 0.91 GJ/t HM	Quader et al. (2016) ⁸ and Keys et al. (2019) ⁷ : added the energy for CCS of 0.91 GJ/t HM	Keys et al. (2019) ⁷
SR+BOF	18.4	9.15	-	21.6	17.8		Shahabuddin et al. (2023) ⁹	Worrell et al. (2007) ⁵	-
SR+BOF+CCS	18.4	9.15	80%	24.89	21.09	36%	same assumption as SR+BOF	Kuramochi et al. (2012) ¹⁰ : added energy for CCS: 3.29 GJ/t HRC * ⁴	Kuramochi et al. (2012) ¹⁰
H2 DRI EAF	16	16	-	12.95	12.95		Vogl et al. (2018) ¹¹	Vogl et al. (2018) ¹¹	-
EW-EAF	12	12	-	12	12		unchanged * ²	unchanged * ²	-
EAF/scrap	7.4	4	-	4.2	2.6		Arens et al. (2017) ⁴	Worrell et al. (2007) ⁵	-

*unchanged: the value is the same as in van Sluisveld et al. (2021); *1: same as van Sluisveld et al. (2021)², who used values from van Ruijven et al. (2016)³; *2: same as van Sluisveld et al. (2021)², who use EC (2016)¹²; *3: 3.37 GJ/ t HRC or 2.57 GJ/ t HRC (considering efficiency improvement of 0.9% over 30 years based on table A-2 in van Sluisveld et al. (2021)² + floor value from BF-BOF (14.8 GJ/t steel) = 17.37 GJ/ t steel; *4: assuming 4.59 GJ / t HRC from Kuramochi et al. (2012)¹⁰ with an efficiency improvement of 1.1% from van Sluisveld et al. (2021)²

1.1.3. Model regions

The IMAGE model distinguishes 26 world regions, as specified in Figure S2 and Table S3. The steel and energy scenarios share the same geographical resolution.

For the LCA model, *premise* creates datasets for each supply chain (e.g., steel production route) in each region. These regionalized supply chains are inputs into regional supply markets (e.g., steel supply in Western Europe). The market mixes are dynamic and derived from the production volume of each production route in the specific region, which is provided by the IMAGE scenario.



Source: PBL 2014

Figure S2: Classification of modelling regions in IMAGE. Countries within each region are provided in Table S3. Source of image: ¹³

Table S3: Countries per modelling regions in IMAGE, with ISO number in parentheses. Source: ¹³. Abbreviations were added.

Region	Abbreviation	Countries (ISO)
Canada	CAN	Canada (124)
USA	USA	St. Pierre and Miquelon (666), United States (840)
Mexico	MEX	Mexico (484)
Central America	RCAM	Anguilla (660), Aruba (533), Bahamas, The (44), Barbados (52), Belize (84), Bermuda (60), Cayman Islands (136), Costa Rica (188), Dominica (212), Dominican Republic (214), El Salvador (222), Grenada (308), Guadeloupe (312), Guatemala (320), Haiti (332), Honduras (340), Jamaica (388), Martinique (474), Montserrat (500), Netherlands Antilles (530), Nicaragua (558), Panama (591), Puerto Rico (630), St. Kitts and Nevis (659), St. Lucia (662), St. Vincent and the Grenadines (670), Trinidad and Tobago (780), Turks and Caicos Isl. (796), Virgin Isl. (Br.) (92), Virgin Islands (U.S.) (850)
Brazil	BRA	Brazil (76)
Rest of South America	RSAF	Argentina (32), Bolivia (68), Chile (152), Colombia (170), Ecuador (218), Falklands Isl. (238), French Guyana (254), Guyana (328), Paraguay (600), Peru (604), Suriname (740), Uruguay (858), Venezuela, RB (862)
Northern Africa	NAF	Algeria (12), Egypt, Arab Rep. (818), Libya (434), Morocco (504), Tunisia (788), Western Sahara (732)
Western Africa	WAF	Benin (204), Burkina Faso (854), Cameroon (120), Cape Verde (132), Central African Republic (140), Chad (148), Congo, Dem. Rep. (180), Congo, Rep. (178), Cote d'Ivoire (384), Equatorial Guinea (226), Gabon (266), Gambia, The (270), Ghana (288), Guinea (324), Guinea-Bissau (624), Liberia (430), Mali (466), Mauritania (478), Niger (562), Nigeria (566), Sao Tome and Principe (678), Senegal (686), Sierra Leone (694), St. Helena (654), Togo (768)
Eastern Africa	EAF	Burundi (108), Comoros (174), Djibouti (262), Eritrea (232), Ethiopia (231), Kenya (404), Madagascar (450), Mauritius (480), Reunion (638), Rwanda (646), Seychelles (690), Somalia (706), Sudan (736), Uganda (800)
South Africa	SAF	South Africa (710)
Western Europe	WEU	Andorra (20), Austria (40), Belgium (56), Denmark (208), Faeroe Islands (234), Finland (246), France (250), Germany (276), Gibraltar (292), Greece (300), Iceland (352), Ireland (372), Italy (380), Liechtenstein (438), Luxembourg (442), Malta (470), Monaco (492), Netherlands (528), Norway (578), Portugal (620), San Marino (674), Spain (724), Sweden (752), Switzerland (756), United Kingdom (826), Vatican City State (336)
Central Europe	CEU	Albania (8), Bosnia and Herzegovina (70), Bulgaria (100), Croatia (191), Cyprus (196), Czech Republic (203), Estonia (233), Hungary (348), Latvia (428), Lithuania (440), Macedonia, FYR (807), Poland (616), Romania (642), Serbia and Montenegro (891), Slovak Republic (703), Slovenia (705)
Turkey	TUR	Turkey (792)
Ukraine region	UKR	Belarus (112), Moldova (498), Ukraine (804)
Central Asia	STAN	Kazakhstan (398), Kyrgyz Republic (417), Tajikistan (762), Turkmenistan (795), Uzbekistan (860)
Russia region	RUS	Armenia (51), Azerbaijan (31), Georgia (268), Russian Federation (643)
Middle East	ME	Bahrain (48), Iran, Islamic Rep. (364), Iraq (368), Israel (376), Jordan (400), Kuwait (414), Lebanon (422), Oman (512), Qatar (634), Saudi Arabia (682), Syrian Arab Republic (760), United Arab Emirates (784), Yemen, Rep. (887)
India	INDIA	India (356)
Korea region	KOR	Korea, Dem. Rep. (408), Korea, Rep. (410)
China region	CHN	China (156), Hong Kong, China (344), Macao, China (446), Mongolia (496), Taiwan (158)
South-eastern Asia	SEAS	Brunei (96), Cambodia (116), Lao PDR (418), Malaysia (458), Myanmar (104), Philippines (608), Singapore (702), Thailand (764), Vietnam (704)
Indonesia region	INDO	East Timor (626), Indonesia (360), Papua New Guinea (598)
Japan	JAP	Japan (392)

Oceania	OCE	American Samoa (16), Australia (36), Cook Isl. (184), Fiji (242), French Polynesia (258), Kiribati (296), Marshall Islands (584), Micronesia, Fed. Sts. (583), Nauru (520), New Caledonia (540), New Zealand (554), Niue (570), Northern Mariana Islands (580), Palau (585), Pitcairn (612), Samoa (882), Solomon Islands (90), Tokelau (772), Tonga (776), Tuvalu (798), Vanuatu (548), Wallis and Futuna Island (876)
Rest of South Asia	RSAS	Afghanistan (4), Bangladesh (50), Bhutan (64), Maldives (462), Nepal (524), Pakistan (586), Sri Lanka (144)
Rest of Southern Africa	RSAF	Angola (24), Botswana (72), Lesotho (426), Malawi (454), Mozambique (508), Namibia (516), Swaziland (748), Tanzania (834), Zambia (894), Zimbabwe (716)

1.1.4. Hydrogen module

The hydrogen supply in IMAGE is represented in an individual module. It includes representations of the production, demand, infrastructure and technology dynamics, supplying hydrogen to all end-use sectors using 12 hydrogen generation technologies. The CAPEX and OPEX costs of these 12 technology options are drawn from the literature^{14,15}. Fuel prices are dynamically represented per technology and region, creating differences in representation and potential across the model. The full parametrisation of the hydrogen module is specified in prior publications^{2,14,15}, while the resulting scenarios are illustrated in section 1.2.5.

1.2. Energy and steel scenarios from IMAGE

1.2.1. Technology mapping

Since we couple the IMAGE steel scenarios with our LCA model, we apply a technology mapping between the two models (see Table S4).

IMAGE distinguishes between “standard,” “efficient,” or “BAT” sub-technologies for some technologies (see BF-BOF and BF-BOF with TGR). For the LCA model, we aggregated these sub-technologies into one technology, BF-BOF and TGR-BF-BOF, using their respective production volumes as weighting factors.

The smelting reduction technology is part of the IMAGE model. However, it does not penetrate the primary steel market in any of the IMAGE scenarios considered. Thus, it is not part of our LCA steel model.

Table S4: Technology mapping between the steel production routes in IMAGE v3.3 and the LCA model in this work.

Steel production route in IMAGE v3.3	Steel production route for the LCA model in this study
Standard BF/ BOF Efficient BF/ BOF	BF-BOF
Standard BF/ BOF + CCS	BF-BOF+CCS
DRI EAF	NG-DRI-EAF
DRI EAF + CCS	NG-DRI-EAF+CCS
Efficient BF/ BOF TGR BAT BF/ BOF TGR	TGR-BF-BOF
BAT BF/ BOF TGR+ CCS	TGR-BF-BOF+CCS
SR+BOF	<i>not modelled since zero production in IMAGE scenarios</i>
SR+BOF+CCS	
H2 DRI EAF	H2-DRI-EAF
EW/EAF	EW
EAF/scrap	scrap-EAF

1.2.2. Regional steel production

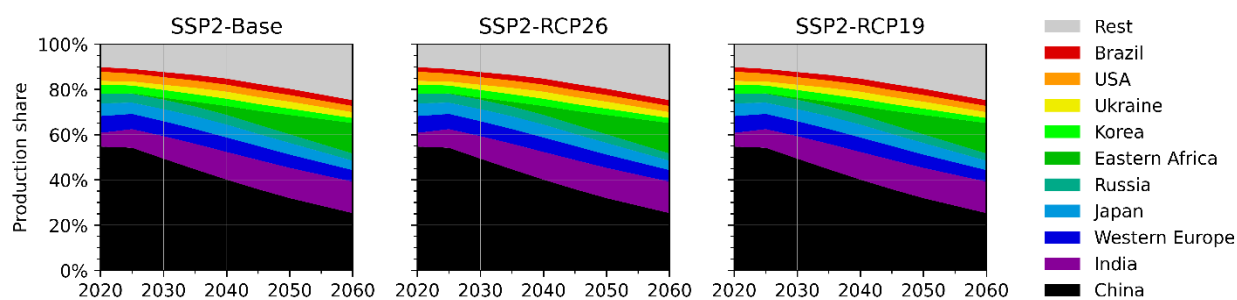
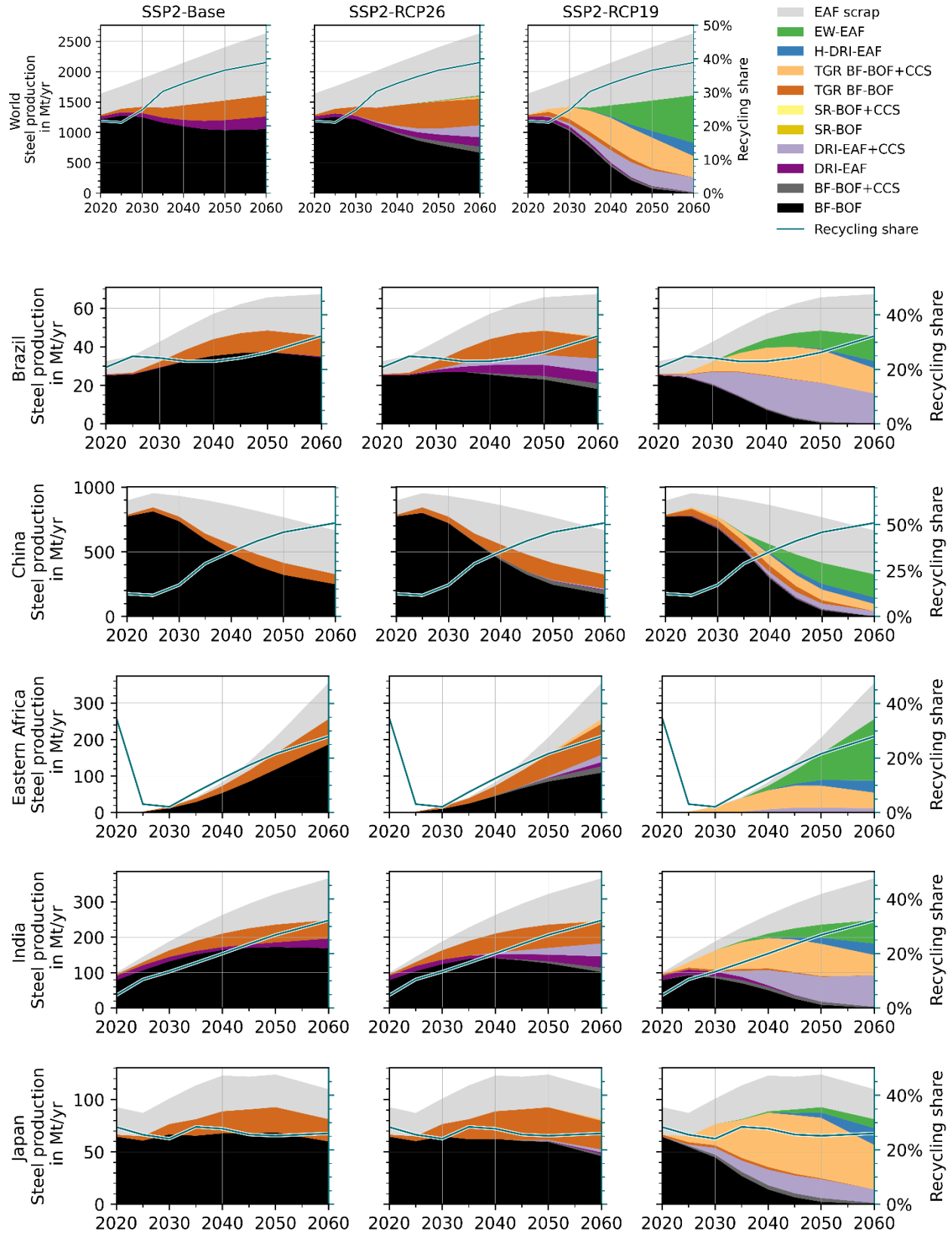


Figure S3: Relative production shares of global steel production in the IMAGE scenarios for the top ten producing regions (based on production volumes in 2040). The category “Rest” aggregates the data for the remaining 16 world regions of IMAGE.

1.2.3. Market mixes of steel production



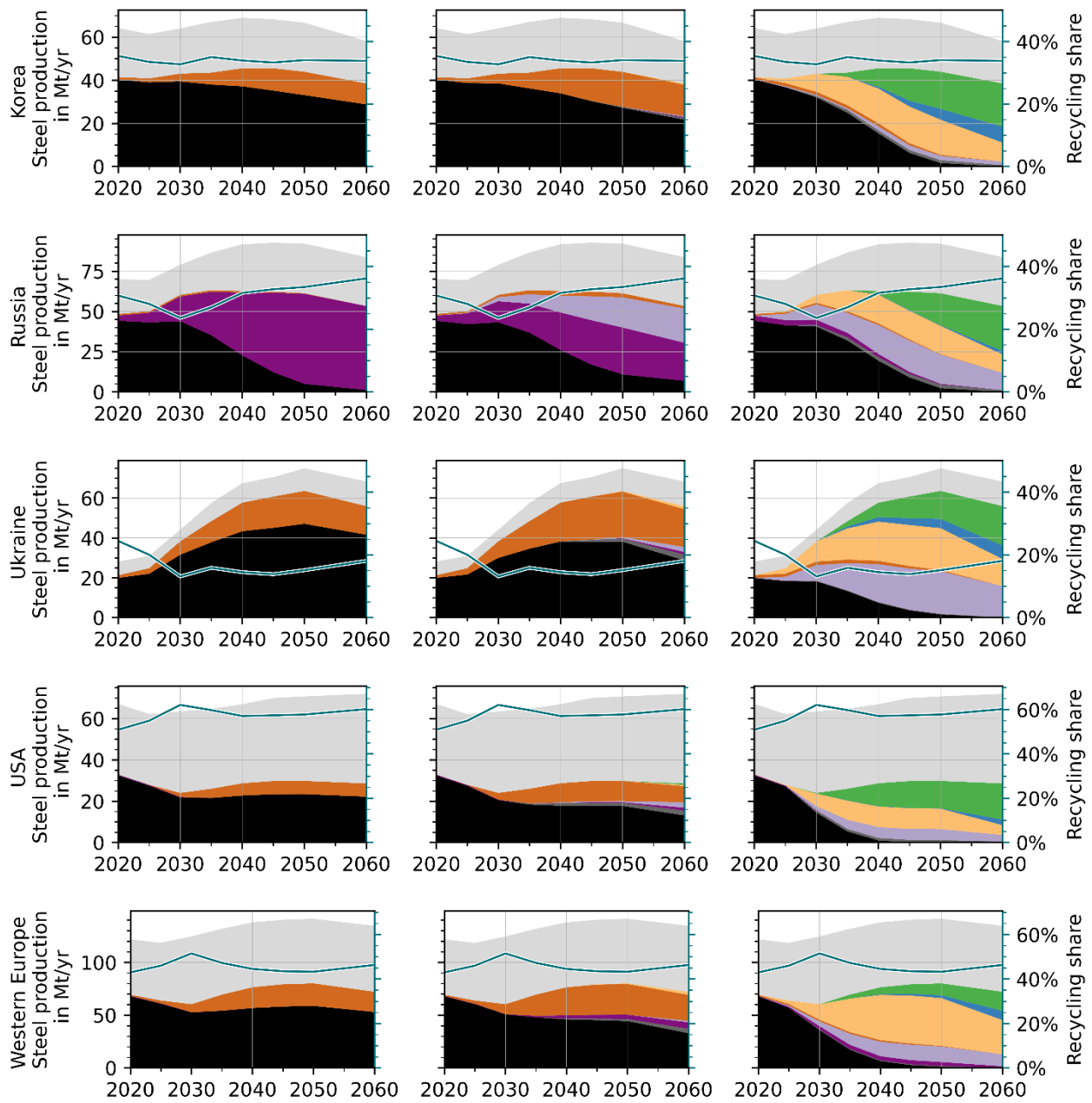
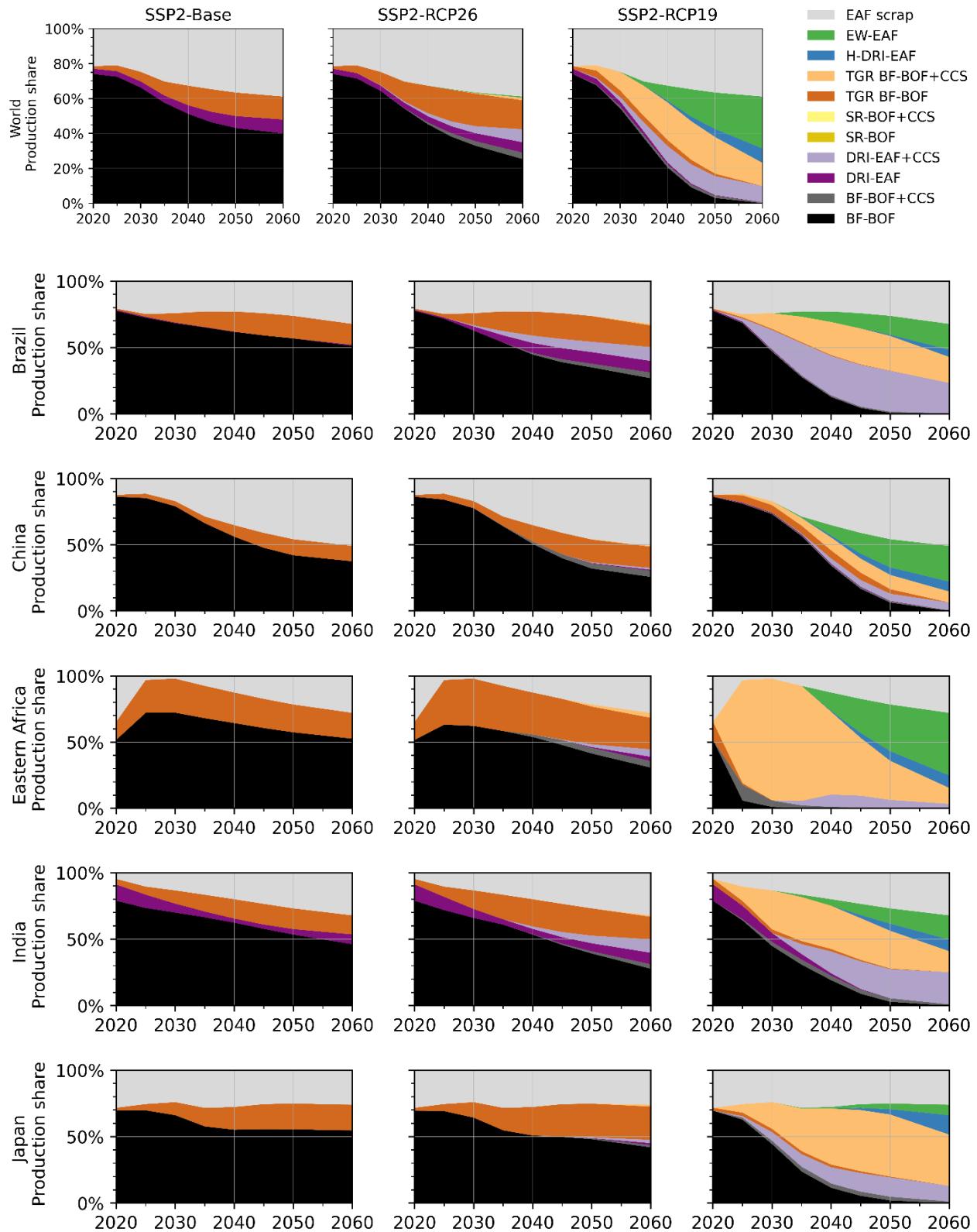


Figure S4: Steel production volumes by production route for the world and the top ten steel producing regions according to the scenarios from IMAGE. Please note the varying y-axis scaling.



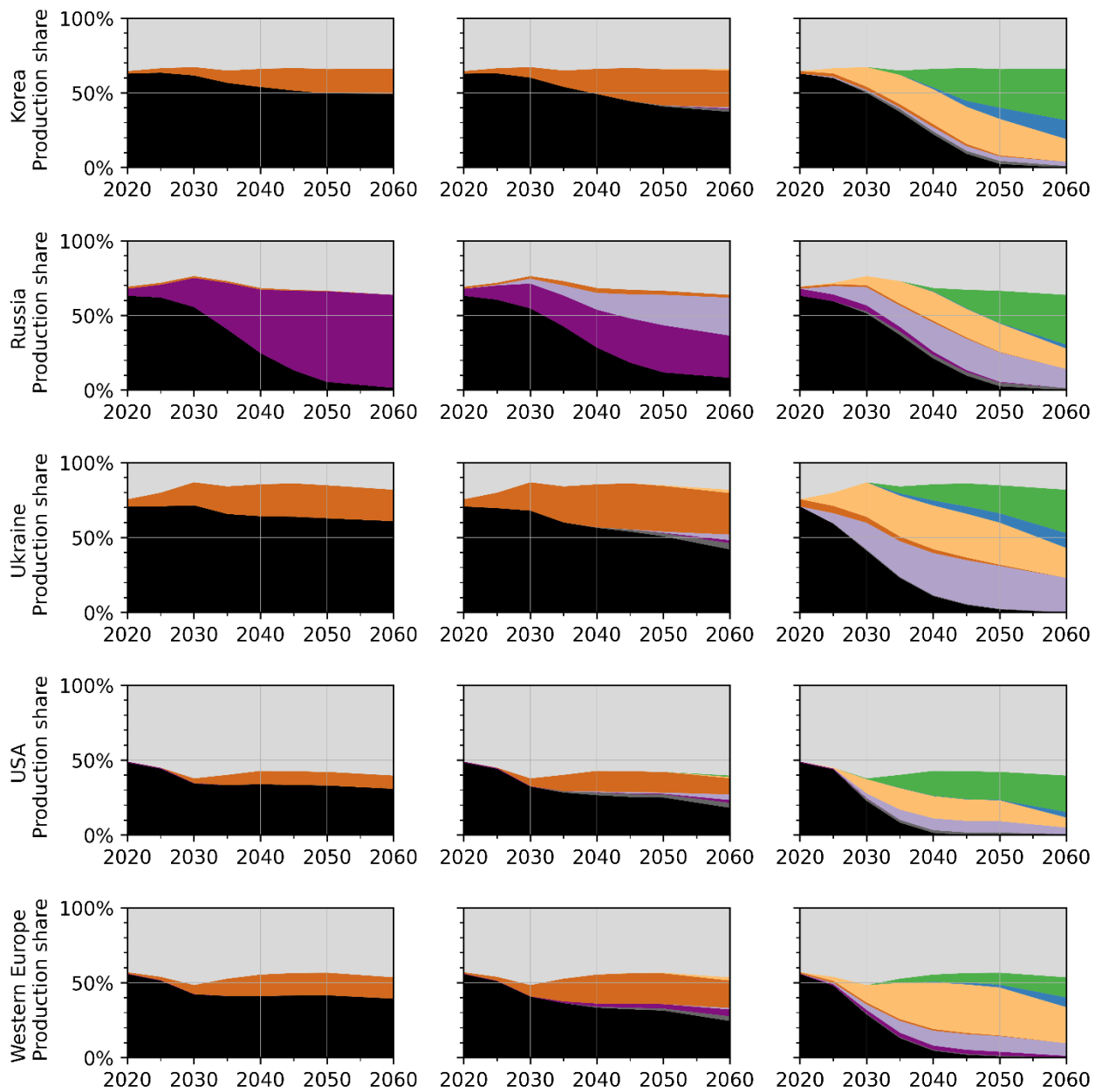


Figure S5: Steel production shares by production route for the world and the top ten steel producing regions according to the scenarios from IMAGE.

1.2.4. Efficiency improvements of iron and steel production

Efficiency improvements are derived from the IMAGE scenarios, specifically, the specific energy consumption (SEC) of each steel production route in each region.

Application to LCIs

Efficiency improvements are applied to iron and steel production processes, such as BF_s, BOF_s, DRIs, or EAF_s (see Figure 2). Thus, other upstream or downstream processes are excluded, such as sinter production, pellet production, or CCS processes.

Generally, they are applied to the entire process, i.e., all inputs, outputs, and emissions. This assumes that efficiency improvements downscale most inputs, outputs and respective emissions equally. Such a downscaling has been applied in previous studies^{16,17} and is a good proxy if a better distinction of inputs and the causal relation to the respective emissions is impossible. Especially in the iron and steel production processes, the high number of inputs, emissions, and their respective cause are unclear. Another complication is that one emission type can be related to several inputs. For example, various carbon-containing energy carriers, and different process-related chemical reactions contribute to one emission type, such as CO₂. But their respective contribution is not documented in the ecoinvent LCA datasets and can thus not be easily adapted.

We excluded certain inputs from the efficiency improvement to ensure correctness of basic material balances. These are inputs of iron-bearing materials (e.g. pig iron, scrap, sponge iron) or alloying elements (e.g. ferronickel, molybdenite, ferrosilicon, or ferromanganese). They are thus kept constant despite efficiency improvements.

Data corrections

The efficiency improvements derived from IMAGE were, to some degree, corrected in two steps based on the following assumptions:

1) technologies can only get more efficient and not less efficient in the future:

- If the specific energy consumption increases in a timestep, which corresponds to an efficiency decrease, it is replaced by the SEC of the previous timestep, such that the SEC (and the efficiency) is kept constant in that timestep.
- This correction follows the same logic as for the efficiency improvements in premise.
- Please note: the correction starts in 2005, as the IMAGE scenario data starts in 2005. Therefore, efficiency improvements only take place in the years when the energy consumption is lower than in 2005.

2) Efficiency improvements cannot exceed a certain annual improvement rate:

- The maximum allowed improvement rate is 1.1%/year based on literature², which corresponds to 36% in total over a time period of 40 years (from 2020-2060).
- If a technology's specific energy consumption (SEC) decreases by more than 1.1 %/year, the maximum improvement rate is applied for that year.
- Thereby, extreme efficiency increases are removed.

The effect of the data correction is illustrated in Figure S6 - Figure S8, while Figure S9 illustrates the final SEC development for the top 10 steel-producing regions.

Original IMAGE data:
Specific energy consumption

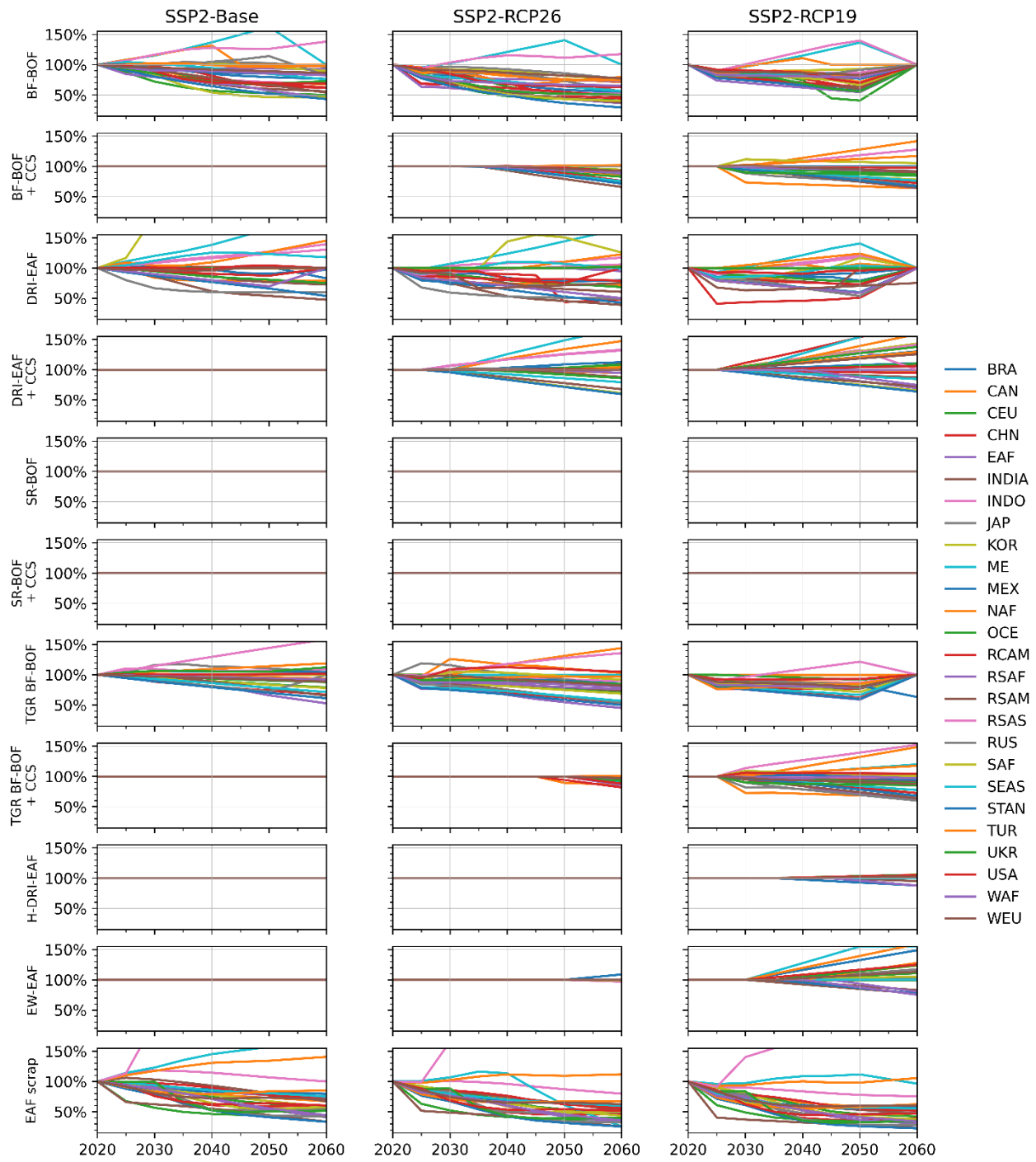


Figure S6: Original IMAGE data of specific energy consumption (SEC) for all steel production routes and regions. Values are relative to 2020. Region abbreviations are provided in Table S3.

Correction 1: increases removed:
Specific energy consumption

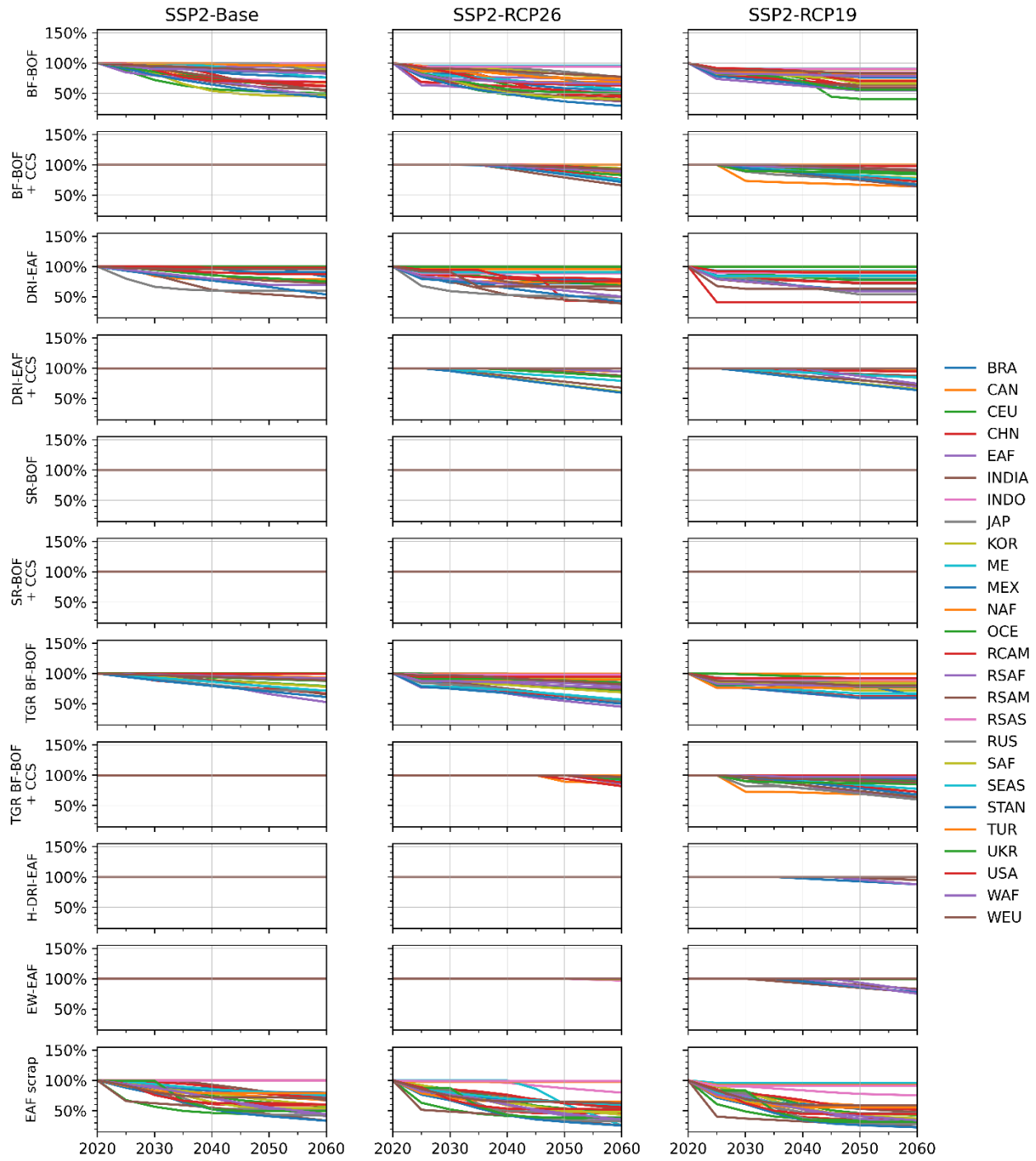


Figure S7: IMAGE data of specific energy consumption for all steel production routes and regions after correction 1, removal of efficiency increases. Values are relative to 2020. Region abbreviations are provided in Table S3.

After all corrections:
Specific energy consumption

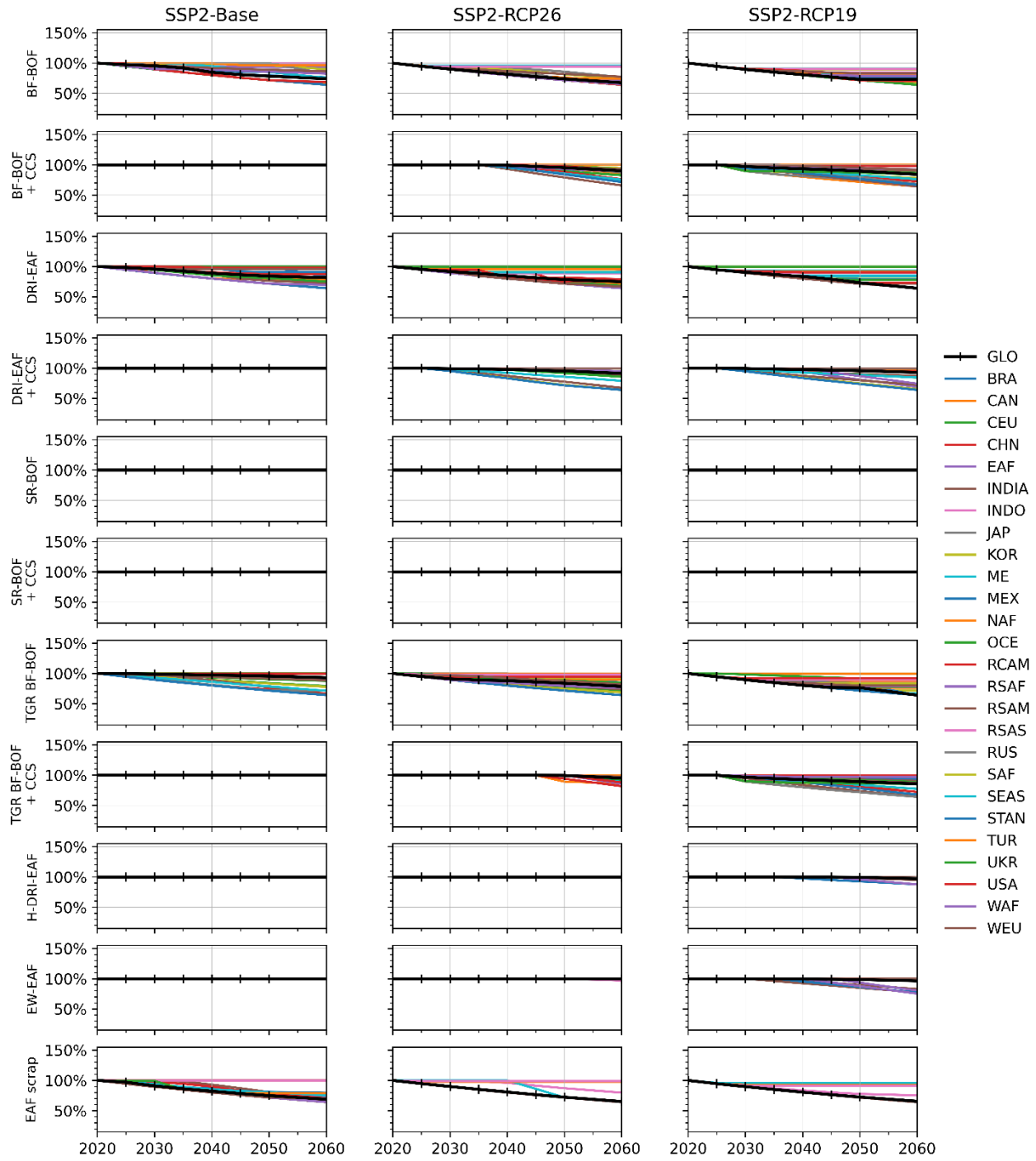


Figure S8: IMAGE data of specific energy consumption for all steel production routes and regions after correction 2, limiting the efficiency increase to a maximum of 1.1%/year. Values are relative to 2020. Region abbreviations are provided in Table S3.

Specific energy consumption

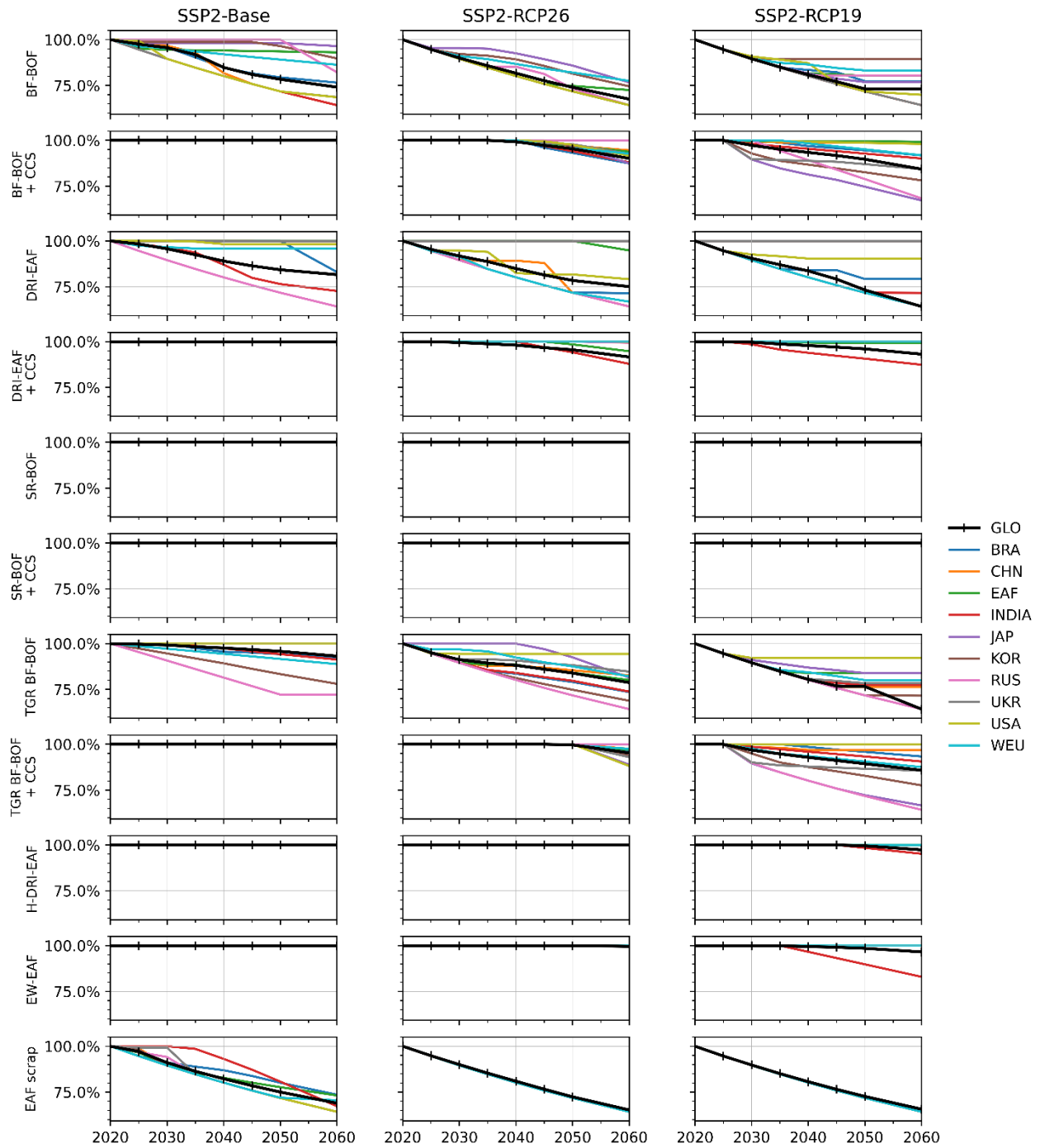


Figure S9: Overview of final specific energy consumption for each steel production route and scenario for the top 10 producing regions. Values are relative to 2020. Region abbreviations are provided in Table S3. While the underlying data in this figure is the same as in Figure S8, this figure shows only the top 10 producing regions. Please note the different scaling of the y-axis.

1.2.5. IMAGE scenario data for energy sectors

Electricity generation in IMAGE

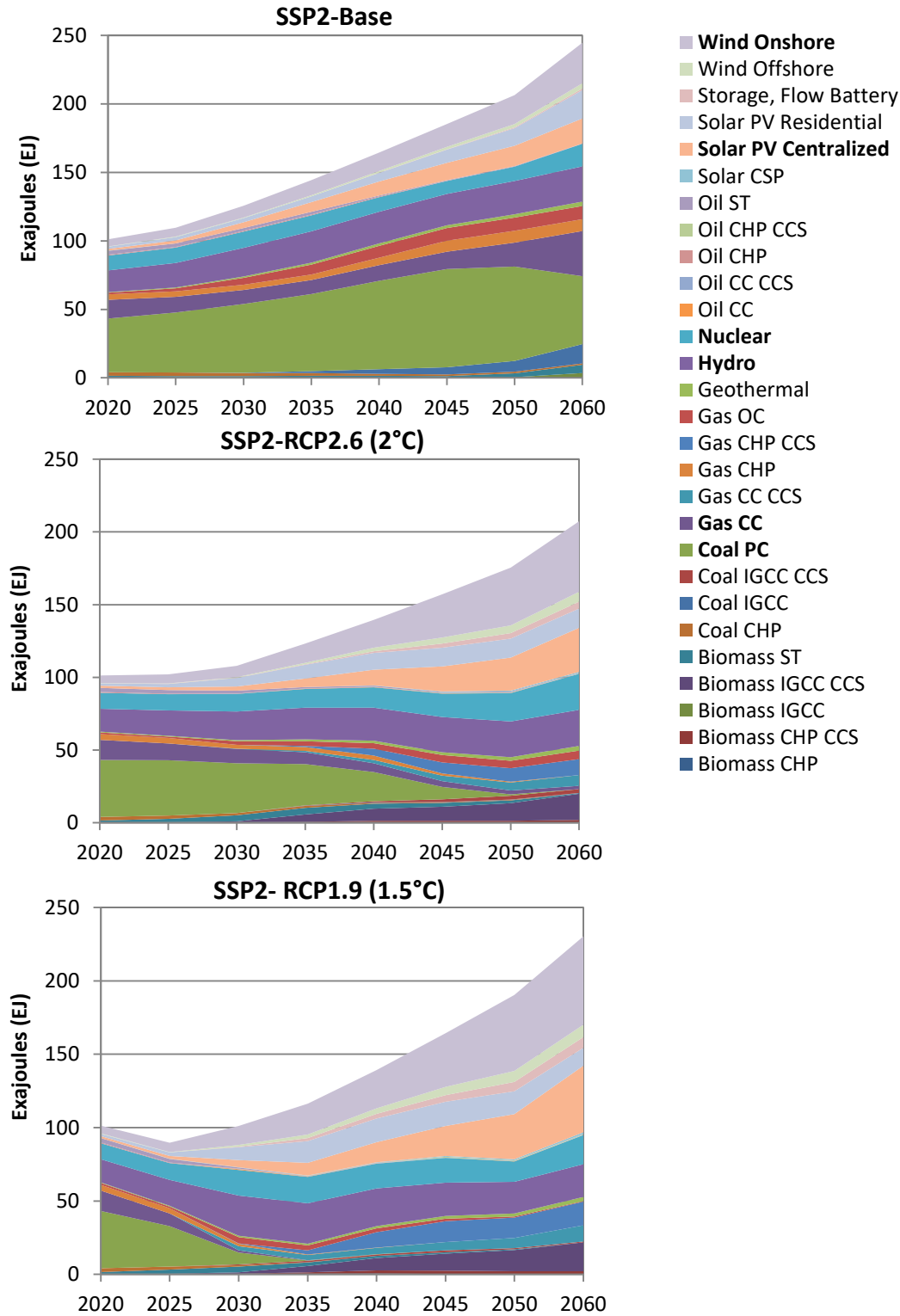


Figure S10: Global electricity generation according to the IMAGE scenarios. Source: premise scenario report.

In all scenarios, global electricity generation more than doubles from 2020 to 2060. In 2020, the share of nuclear power was 11%, generating 10.9 EJ of global electricity demand. It increases to 16.4 EJ in the Base

scenario, to 24.7 EJ in the 2°C, and to 19.8 EJ in the 1.5°C scenario, contributing to power generation in 2060 with a share of 7%, 12% and 9% respectively. Thus, in all scenarios, global capacities for nuclear power are considerably expanded, although the degree shows variations depending on the scenario (ranging from a factor of 1.5 to 2.3).

For power generation with CCS applied, the share in 2020 is 0%. CCS is not considered in the Base scenario, but in the other two scenarios. It is deployed to 20% and 22% of power generation technologies by 2060 in the 2°C and 1.5°C scenarios respectively, with the largest shares originating from Biomass IGCC CCS (9% and 8% respectively), followed by Gas CC CCS (4% and 5% respectively) and Gas CHP CCS (5% and 7% respectively). Oil-based generation with CCS is not at all used.

Hydrogen generation in IMAGE

Depending on the scenario, hydrogen is primarily generated from natural gas for SSP2-Base and natural gas with CCS for SSP2-RCP2.6 (see Figure S11). Only in SSP2-RCP1.9, renewable generation (i.e., from solar and electrolysis) contributes to the mix, but supplies still in sum less than 15%. The majority is still natural gas-based with CCS. As the CAPEX and OPEX costs are significantly higher for green hydrogen than for the other technology options, green hydrogen technologies cannot be adopted cost-effectively at a large scale without some enforced share, i.e., narrative-driven choices.

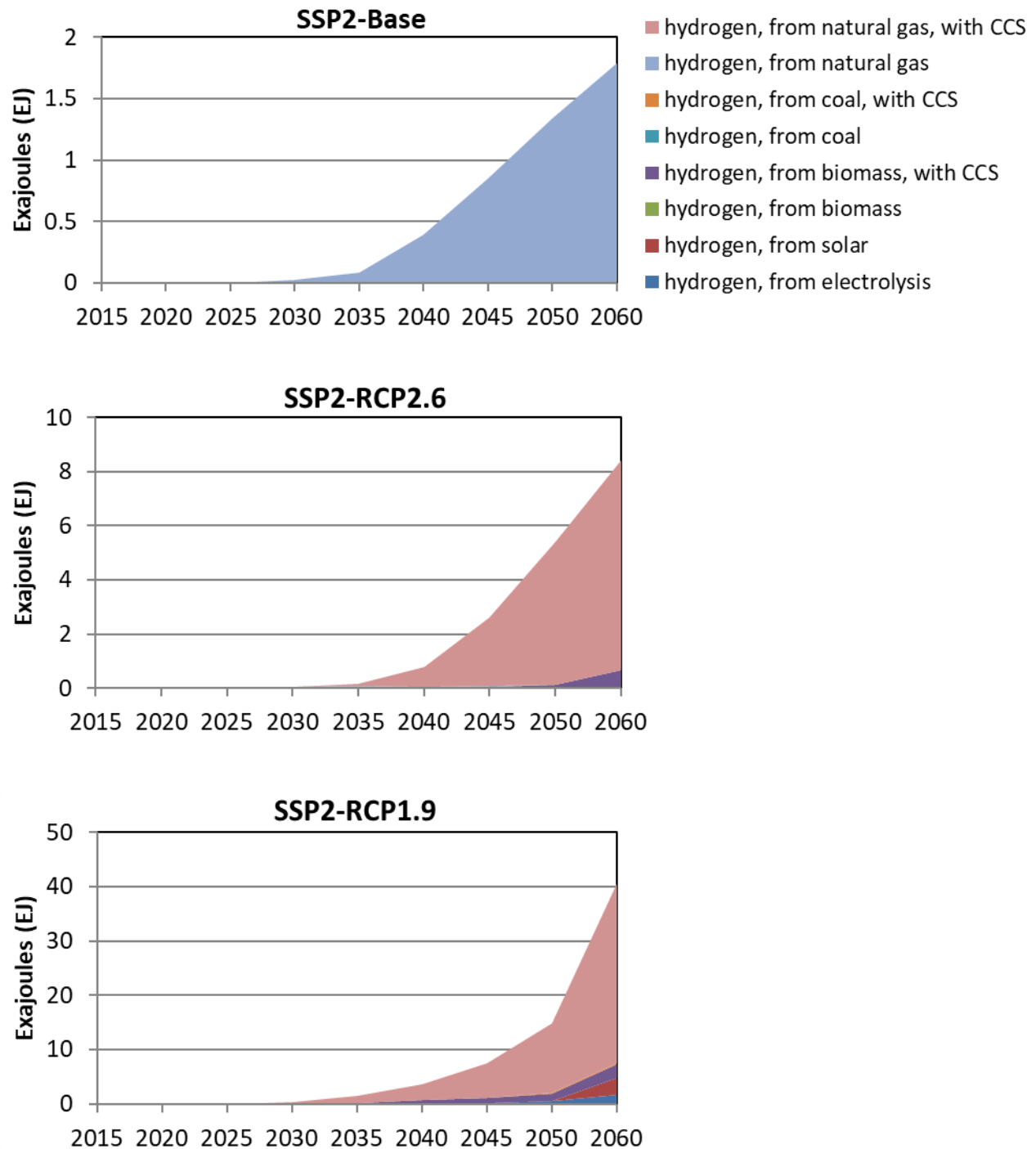
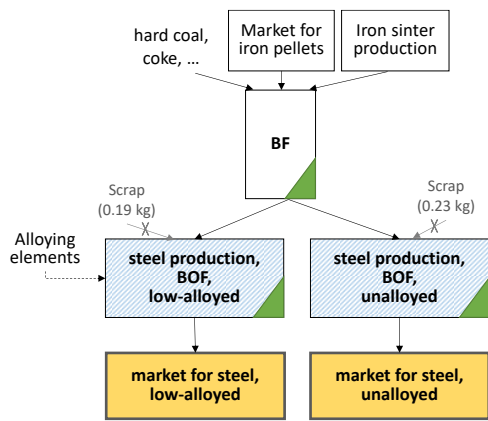


Figure S11: Global hydrogen generation according to the IMAGE scenarios (note the varying y-axis). Source: Premise scenario report.

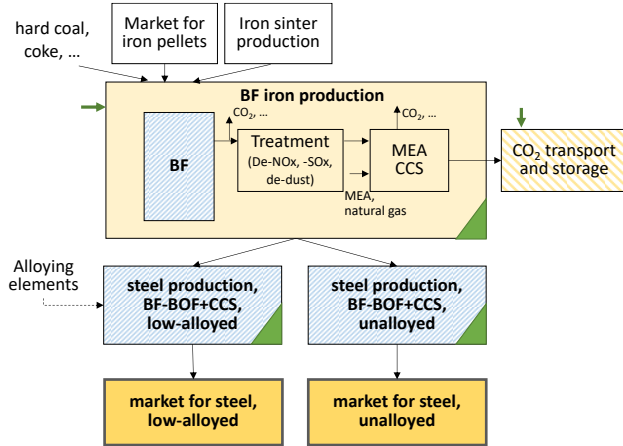
1.3. Life Cycle Inventories

The LCIs are provided in the repository in an excel workbook, where they are documented¹⁸. Details and values can be extracted from there. Here, we provide an overview about the main modelling assumptions, data sources and, if required, some additional calculations.

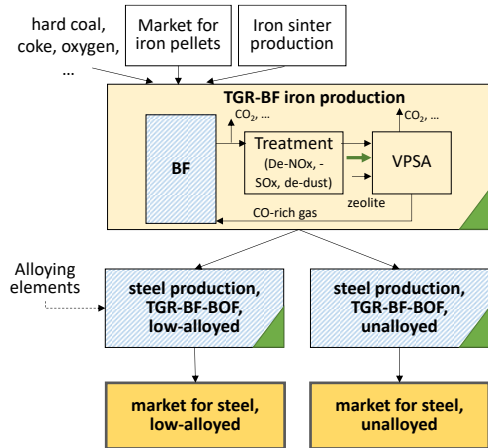
a) BF-BOF



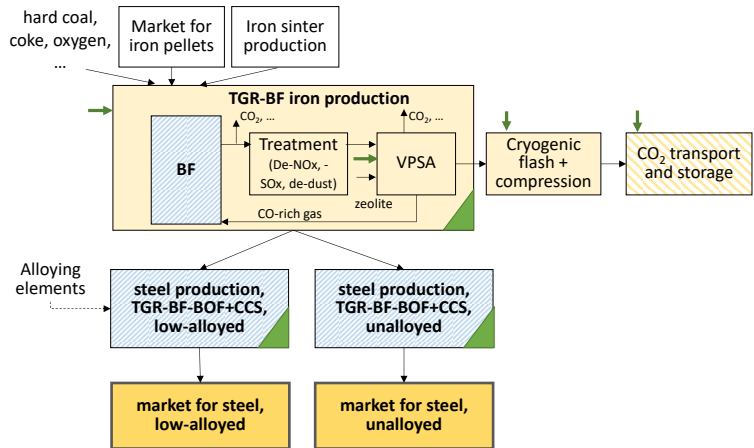
b) BF-BOF-CCS



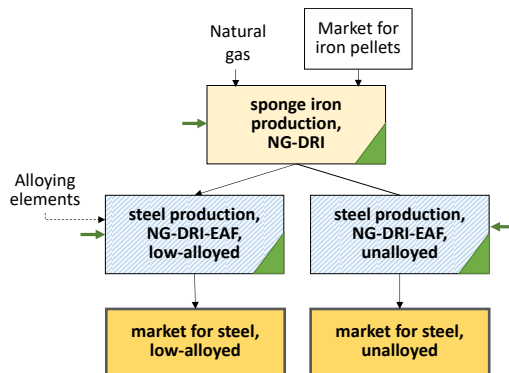
c) TGR-BF-BOF



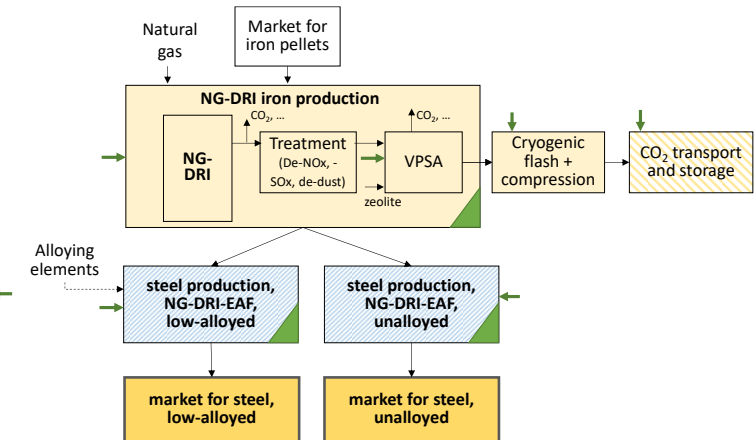
d) TGR-BF-BOF+CCS



e) NG-DRI



f) NG-DRI +CCS



g) H2-DRI

h) EW

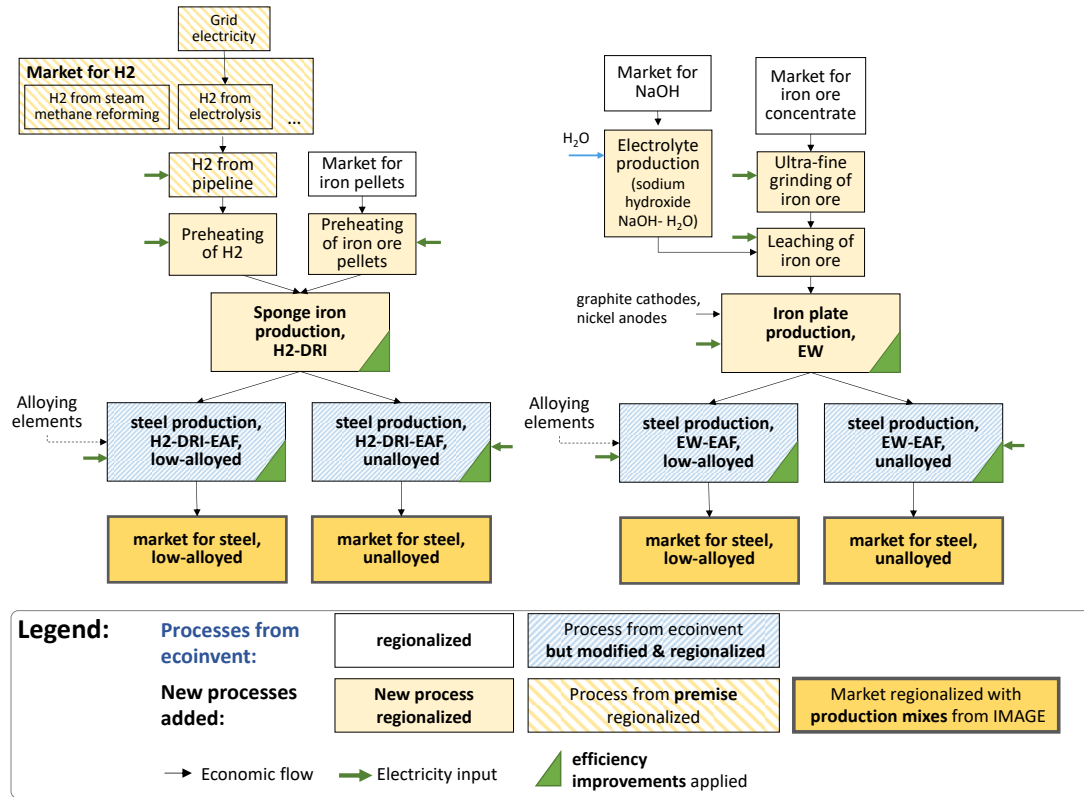


Figure S12: Simplified flowcharts of the LCIs for the modelled primary steel production routes. Regionalization means that the processes are regionalized into the IAM regions.

Table S5: General assumptions for LCIs for steel production processes.

	Assumptions and adaptations	Process basis	Applies to
BF	Process from ecoinvent but adapted if used in other production routes than BF-BOF, see respective other routes.	Ecoinvent 3.9.1: process: "pig iron production" reference product: "pig iron" region: "RER"	BF-BOF BF-BOF+CCS TGR-BF-BOF TGR-BF-BOF+CCS
BOF	Process from ecoinvent, but adapted: 1) removed input of scrap, instead source the input from the respective preceding BF process 2) removed input of secondary metallurgy slag, and added the amount to the BOF slag 3) source iron from the respective preceding BF process These adaptations aim to make the BOF more representative for primary production and the respective production route.	Ecoinvent 3.9.1: process: "steel production, converter, low-alloyed" product: "steel, low-alloyed" region: "RER"	BF-BOF BF-BOF+CCS TGR-BF-BOF TGR-BF-BOF+CCS
TGR-BF	Process from ecoinvent, but adapted: VPSA is used to separate CO ₂ from the CO-rich gas from the BF top gas, such that the CO-rich gas can be recirculated to the BF. 1) reduced inputs of coke and hard coal: -24.5% ⁸ 2) reduced CO ₂ emissions: -24% ⁸	Ecoinvent 3.9.1: process: "pig iron production" reference product: "pig iron" region: "RER"	TGR-BF-BOF

	<p>3) reduced emissions of particulate matter: -24.5% (assumption: same rate as for coke and hard coal)</p> <p>4) reduced CO emissions: -90%⁸ (top gas recycling ratio)</p> <p>5) reduced SO₂ and NO_x emissions due to gas treatment of VPSA: -95% and -100% respectively^{7,19}</p> <p>6) additional requirement for oxygen: 0.08316 kWh/kg pig iron ²⁰ (instead of hot air blast, pure oxygen is injected into the furnace to reduce nitrogen and to increase the CO and CO₂ concentration in the top gas^{10,20}</p> <p>7) additional requirement for electricity for operation of the VPSA ²⁰</p> <p>8) additional zeolite requirement as adsorbent for VPSA: 1.7 kg zeolite/ t CO₂ separated ¹⁹</p>		
NG-DRI	DRI is assumed as a natural gas-based process, since for current DRI processes, the vast majority is operated with natural gas using shaft furnaces ²¹ .	Modelled based on data from Nduagu et al. (2022) ²²	NG-DRI
H2-DRI	<p>Based on Li et al. (2022)²³, but adapted:</p> <p>1) added losses of hydrogen due to purging of top gas, which increases the theoretical stoichiometric H2 demand of 580 m3/t DRI²³ by 20%²⁴ to 633 m3/t DRI (hydrogen makeup). The gas inflow into the furnace is much higher, but the top gas of the furnace is recirculated and its remaining hydrogen remixed into the gas for the furnace ^{23,24}.</p> <p>2) added electrical preheating of hydrogen and the gas inflow into the furnace of 0.23 MWh/t DRI²⁴ or 4.02 kWh/kg H2 consumed. The preheating is not only for the hydrogen consumed, but for the entire gas inflow into the shaft furnace. This gas inflow is considerably higher (by a factor of 2.5²⁴ to 3.8²³) than only the hydrogen consumed, as additional hot gas is required to provide heat for the endothermic reaction in the furnace, i.e. reducing iron oxide with H2. Assumptions: 633 m3 H2 consumed /t DRI (equal to 0.057 kg H2 consumed/kg DRI); 1600 m3 gas inflow into furnace/t DRI; conversion factor for H2: 0.09 kg H2/m3 H2; temperatures for the inflow into the shaft furnace: 930-940°C^{23,24}.</p> <p>3) added preheating of iron ore pellets before they enter a shaft furnace based on Bhaskar et al. (2020)²⁵, using an electrical heater of a thermal efficiency of 0.85.</p> <p>4) hydrogen is sourced from the average regional market for hydrogen based on IMAGE scenarios which includes hydrogen distribution by pipeline and geological storage.</p>	Modelled based on data from Li et al. (2022) ²³	H2-DRI, (green H2-DRI is described below)
EW	The main data sources for the processes of electrowinning are Siderwin (2020) ²⁶ , EC (2016) ²⁷ , Lavelaine (2019) ²⁸ . Where necessary, additional data was extracted from ecoinvent as proxies to fill data gaps.	Modelled based on data from Siderwin (2020) ²⁶ , EC (2016) ²⁷ , Lavelaine (2019) ²⁸ , Zhao et al. (2020) ²⁹ , and various	EW

	More details about the sub-processes are provided below in section 1.3.1.	processes from ecoinvent.	
EAF	<p>Process from ecoinvent, but adapted: The adaptations aim to make the EAF more representative for primary instead of secondary production:</p> <ol style="list-style-type: none"> 1) removed input of scrap, instead source the input from the respective preceding iron production process 2) Entire process is downscaled by 1 parameter to produce 1 kg of steel from primary sources instead of scrap iron: 0.9369, leading to 1.06 kg iron / 1 kg steel. This value has been reported for DRI-EAF²⁵ and EW-EAF²⁶. The parameter is applied to all inputs and outputs. 3) removed input of secondary metallurgy slag, and added the amount to the EAF slag 	Ecoinvent 3.9.1: process: "steel production, electric, low-alloyed" reference product: "steel, low-alloyed" region: "Europe without Switzerland and Austria"	NG-DRI NG-DRI+CCS H2-DRI EW
Scrap-EAF	<p>Process from ecoinvent, but adapted for those regions where the EAF receives pig iron or sponge iron as input instead of only iron scrap: sponge iron and pig iron input are set to zero, and their amounts are replaced with iron scrap to make the EAF more representative for secondary production.</p>	Ecoinvent 3.9.1: process: "steel production, electric, low-alloyed" reference product: "steel, low-alloyed"	scrap-EAF

1.3.1. Electrowinning

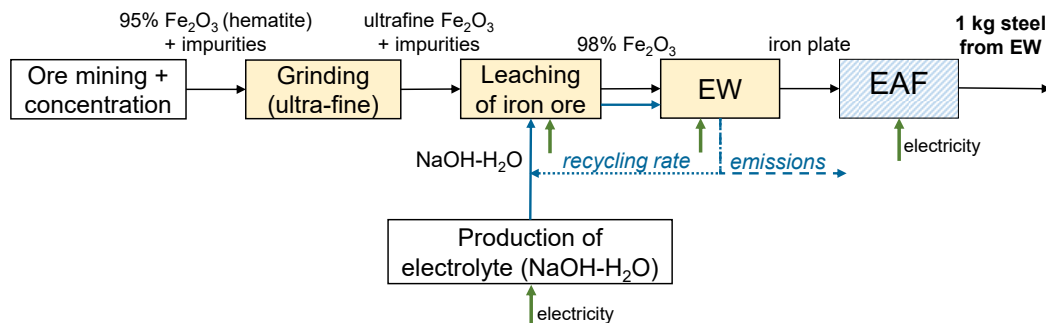


Figure S13: Flowchart for electrowinning based on Siderwin (2020)²⁶ and adapted.

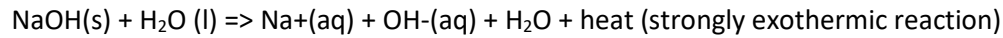
Electrowinning (iron plate production)

The process produces an iron plate via electrolysis of iron ore and is based on the following assumptions:

- Low-temperature electrowinning at 110°C of iron from an alkaline solution (sodium hydroxide and water) at 1.7 Volt²⁶.
- The input is 98% iron oxides (Fe₂O₃), which are deposited at the cathode during the process, such that iron plates are produced. The anode attracts the oxygen which flows up as gas. Based on the mass balance published by EC (2016)¹², the iron plate still contains 2% impurities.
- No CO₂ emissions occur during the process¹².

Emissions to water of hydroxide, sodium ions and water:

We assume the used electrolyte of NaOH-H₂O (sodium hydroxide dissolved in water with 50 wt-%) is not recycled. NaOH is very soluble in water. It will split into Na⁺ and OH⁻ once in contact with water, according to the following reaction:



Therefore, we assume that the used sodium hydroxide solution is released into water as sodium ions, hydroxide (OH⁻) and water. The amounts of these emissions are calculated stoichiometrically.

Electricity consumption:

- 2.392 kWh/kg iron plate ²⁶

Ecoinvent processes used:

Processes required for leaching and EW are similar to aluminium production, specifically, the Bayer process, which is used for alumina extraction from Bauxite²⁶. Therefore, data gaps are filled using proxies from ecoinvent from the process "aluminium production, primary, liquid, prebake", e.g. for:

- o input of aluminium electrolysis facility construction
- o cathode requirement

Anode:

- Nickel anodes, as in water electrolysis, are assumed³⁰
- Lifetime: 10 years^{29,31} for hydrogen electrolysis using an alkaline electrolysis cell (AEC)
 - o Nickel anode required per m² AEC: 1.135 kg Ni-anode / m² AEC²⁹ for hydrogen AEC
- Production amounts: 50 kg Fe/day using 3 m² cell as in the Siderwin project²⁸

$$\frac{1.135 \frac{\text{kg Ni - anode}}{\text{m}^2 \text{ AEC}}}{50 \frac{\text{kg Fe - plate}}{3 \text{ m}^2 \text{ day}} \cdot 10 \text{ years} \cdot 365 \frac{\text{days}}{\text{year}}} = 1.86 \cdot 10^{-5} \frac{\text{kg Ni - anode}}{\text{kg Fe}}$$

Leaching of iron ore

Leaching is assumed to be similar to the Bayer process for aluminium production from bauxite²⁶. An alkaline solution (sodium hydroxide, NaOH-H₂O) is used to remove gangue through precipitation of silicon aluminate via quick lime. As a result, the ultrafine iron ore (95% hematite) can be purified to 98% iron oxide (Fe₂O₃).²⁶

The process requires 0.13 kWh of electricity per kg of iron oxide (based on Ref²⁶, Figure 4.2: 200 kWh / 1537 kg).

Electrolyte (alkaline solution) requirements:

- based on Ref ¹², we assume: 40 wt-% Fe₂O₃ in 50 wt-% NaOH-H₂O, at 110°C, which means that 60 wt-% is the NaOH-H₂O solution
 - o Density NaOH-H₂O at 100°C and 50wt%: 1.47 kg/ litre
- mass-ratio solution vs. Fe₂O₃: $m_{\text{NaOH-H}_2\text{O}} = 1.5 \cdot m_{\text{Fe}_2\text{O}_3}$
- Since this is for electrowinning, we assume here: $m_{\text{Fe}_2\text{O}_3} = 1537 \text{ kg}$ (i.e. 98% purity + 2% impurities)²⁶:

$$\rightarrow m_{\text{NaOH-H}_2\text{O}} = 1.5 \cdot m_{\text{Fe}_2\text{O}_3} = 1.5 \cdot 1537 \text{ kg} = 2305.5 \text{ kg for producing 1085 kg iron plate}$$

$$\rightarrow 2305.5 \text{ kg electrolyte} / 1085 \text{ kg iron plate} = 2.125 \text{ kg electrolyte / kg iron plate}$$

The recycling rate of the alkaline solution is unknown. It is stated that the sodium hydroxide gets recirculated in the system.

- If recycling rate = 0% → 1.5 kg solution / kg Fe₂O₃
- If recycling rate = 50% → 0.75 kg solution / kg Fe₂O₃

We assume a conservative recycling rate of 50%, thus 0.75 kg of alkaline solution/kg of iron oxide.

Ultra-fine grinding of iron ore

- Grinding of iron ore (as used for input for pellets of size F80 of 60µm) to ultra-fine iron ore (output mineral particle size has a P80 of 10µm²⁶).
- The concentration of the hematite (Fe₂O₃) input is 95%. This corresponds to 66% Fe in iron ore, which is very similar to the ecoinvent process of iron ore beneficiation, where milling also takes place.
- Electricity consumption: 0.063 kWh/kg²⁶
- Additional inputs of industrial machine, conveyor belt and heat (for heating of buildings) are assumed to be the same as in the ecoinvent 3.9 process of: quicklime production, milled, loose (CH)
- Dust emissions are assumed to be negligible. This is also assumed for the ecoinvent process of milling quicklime.

Electrolyte production (sodium hydroxide)

- An alkaline solution is produced, i.e. NaOH-H₂O, with 50 wt-% sodium hydroxide¹².
- The source of sodium hydroxide is the global market for sodium hydroxide from ecoinvent, since this includes three different production routes.
 - o This market provides sodium hydroxide at 50% solution state but without water. Thus, the same amount of water is added to produce NaOH-H₂O with 50 wt-% of sodium hydroxide.

1.3.2. Carbon capture and storage processes

The production routes including CCS are modelled using the respective base production route but then include additional CCS processes. The main assumptions of those CCS processes are specified in Table S6 and explained below.

BF-BOF-CCS

BF-BOF-CCS uses mono-ethanolamine (MEA) as an absorbent. The CCS process is based on Müller et al. (2024)³², but modified for the application to capturing emissions from steel production (see Table S6):

- natural gas is used for regenerating MEA⁶
- added the respective CO₂ emissions of the natural gas consumption
- added the input of activated carbon for the removal of degraded amine: 0.06 kg/t CO₂^{19,33}

Gas pre-treatment for CCS reduces emissions of particulate matter¹⁹, NO_x³⁴, and SO₂³⁴ (see Table S6).

TGR-BF-BOF+CCS

TGR-BF-BOF already includes the VPSA to separate CO₂ from the CO-rich gas from the top gas. However, the CO₂ gas from the VPSA is unsuitable for CO₂ transport and storage. Therefore, additional processing is required to increase the purity and pressure of the CO₂ gas, which is modelled via cryogenic flash and compression^{7,8}. The last process is CO₂ transport and storage.

NG-DRI+CCS

NG-DRI+CCS applies the same sub-processes as TGR-BF-BOF+CCS for gas pre-treatment, CO₂ separation via VPSA and the subsequent cryogenic flash, compression, and CO₂ transport and storage.

Table S6: Technology data and data sources for CCS technologies of steel production routes.

	BF-BOF+CCS (MEA)	TGR-BF-BOF+CCS (VPSA)	NG-DRI+CCS (VPSA)
Process basis	Ecoinvent 3.9.1.: "pig iron production" - reference product: "pig iron" - region: "RER"		Nduagu et al. (2020) ²²
Direct CO₂ emissions of iron process in 2020 kg CO ₂ /kg iron	0.85 (ecoinvent)	0.645 (-24% of BF) ⁸	0.51 Nduagu et al. (2020) ²²
Carbon captured in 2020 kg CO ₂ / kg iron	0.71	0.44	0.48
Carbon capture rate	-54% of direct emissions of the BF-BOF route ⁶	-52% of direct BF emissions through CCS via VPSA ⁸	-94% of direct DRI emissions ⁷
CCS energy penalty MJ/kg CO ₂ captured	2.71 natural gas ⁶ for heat for MEA regeneration	0.67 electricity ⁸ for cryogenic flash and compression	1.05 electricity ⁸ for VPSA and cryogenic flash and compression
Emission reduction rates			
NO_x	-80% ³⁴	-100% ¹⁹	-100% ¹⁹
SO₂	-100% ³⁴	-95% ¹⁹	-95% ¹⁹
Particulate matter	-50% ¹⁹	-50% (assumption: as MEA ¹⁹)	-50% (assumption: as MEA ¹⁹)
CO₂ transport and storage	Process used from premise, which is based on Volkart et al. (2013) ³⁵		

1.3.3. Green H2-DRI

For H2-DRI, the hydrogen is sourced from the regional hydrogen market, which is governed by the IMAGE scenarios. It thus includes a wide range of hydrogen generation technologies, e.g. natural gas-based steam methane reforming (see section 1.2.5). In a sensitivity analysis, we assume green hydrogen for the iron production. The green hydrogen is sourced from PEM electrolyzers operated with renewable electricity only, i.e., electricity from onshore wind turbines (1-3 MW).

The dataset for green hydrogen from PEM electrolyzers is based on the dataset in premise, but electricity from the grid was replaced with electricity from wind power.

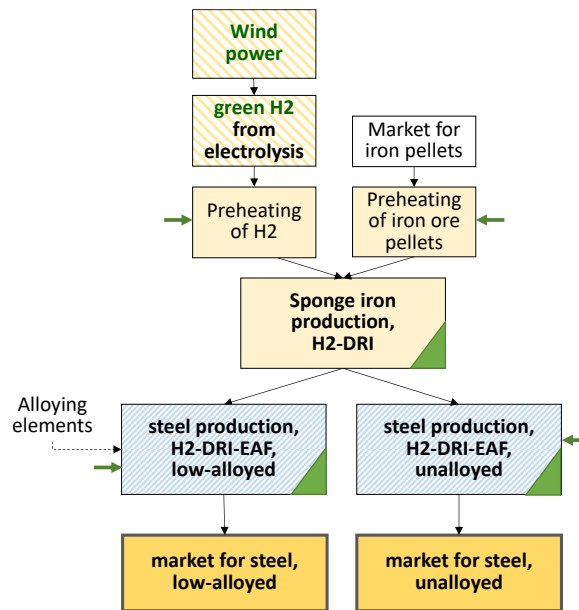


Figure S14: Simplified flowchart for green H2-DRI.

1.4. Integration of scenario data into ecoinvent

1.4.1. Premise

For importing LCIs and integrating energy and steel scenarios into ecoinvent, premise was used. Specifically, the following version was used:

- Version: 2.1.1.dev4
- Last commit from June 28, 2024:
 - o <https://github.com/polca/premise/commit/caeb4809ab7002cf7ad1f703afa768f79217beae>
 - o Commit hash: caeb4809ab7002cf7ad1f703afa768f79217beae

For version 2.1.1, scenarios for heat have been added. This means that the fuel mixes for heat-supplying datasets are based on the regional fuel mix. For example, the fuel mix of a gas boiler might change from natural gas to a mix of biogas and synthetic gas.

1.4.2. Creation of regional steel markets

Ecoinvent 3.9.1. contains production processes and supply chains for six different steel types: unalloyed, low-alloyed, chromium, reinforcing steel, hot-rolled low-alloyed and hot-rolled chromium steel. We implement our new production routes and scenarios for all steel types to cover the entire steel supply chain within the database. Exceptions are chromium steel, which is produced only via the EAF, and reinforcing steel, which is produced from unalloyed and low-alloyed steel (see Figure S15). Moreover, hot-rolled steel is manufactured by a subsequent hot-rolling process, which applies to low-alloyed and chromium steel.

For each steel type, the respective steel production routes are regionalized into all 26 IMAGE regions. These serve as input for a respective regional market for each steel type (see Figure S15), using the steel production mix as in the IMAGE scenario. Additionally, a world market is created for each steel type based on the total production amount of each region.

Lastly, a global market group for steel summarises the global steel production from all six steel types based on their global markets, as described below, section 1.4.3.

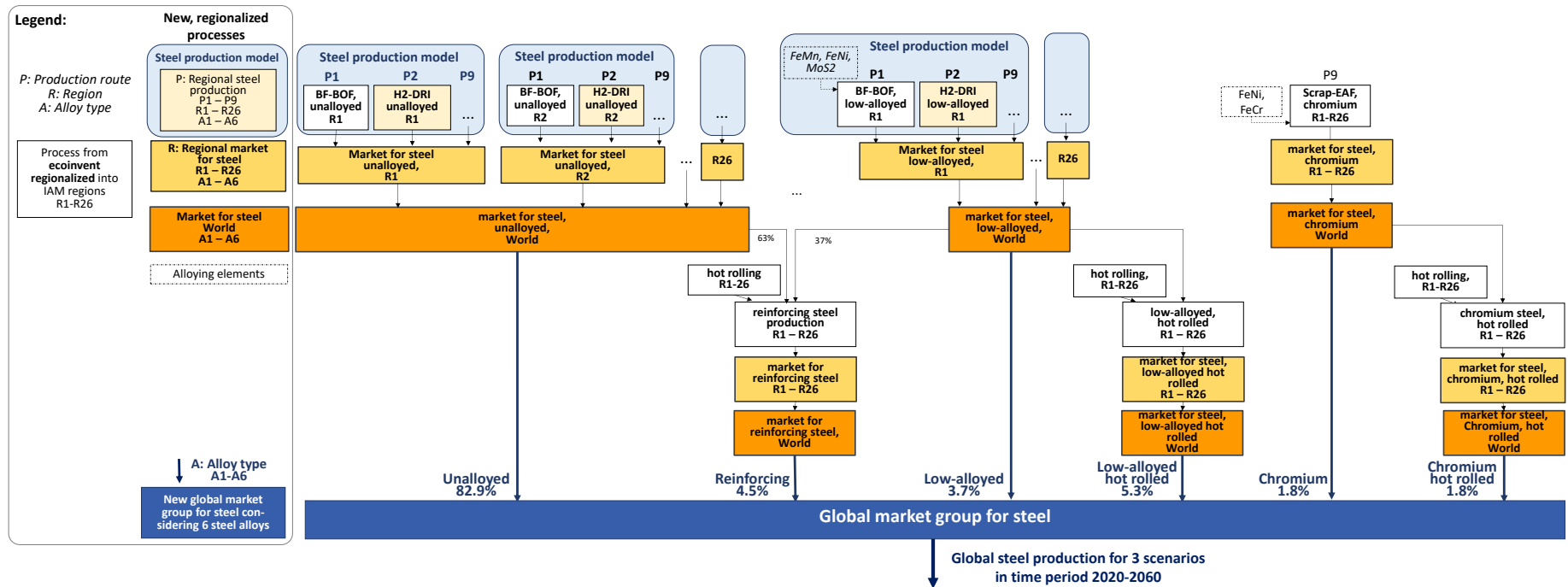


Figure S15: Composition of the regional and global steel market for all six steel types.

1.4.3. Creation of a global market group for steel

As shown in Figure S15, the global market group for steel aims to represent the global steel production with the six steel types available in ecoinvent. The production shares of each steel types are assumed to be constant due to a lack of scenario data. We assume production shares based on data from ecoinvent, i.e. the production amounts for the different steel types (see Table S7).

Since reinforcing steel is produced from unalloyed and low-alloyed steel by additional hot rolling (Figure S15), we correct the total production amount accordingly to calculate the production share of unalloyed and low-alloyed steel.

Chromium and low-alloyed steel can be additionally hot-rolled to produce hot-rolled steel. According to the production volumes stated by ecoinvent, 50% of their production undergoes hot rolling.

The total annual steel production of 1.5 Gt based on ecoinvent data is in the same order of magnitude as in the IMAGE data for 2020, which is about 1.6 Gt of steel.

Table S7: Production amount of steel markets in ecoinvent, which is used to create a global steel market considering six different steel types. 50% of chromium and low-alloyed steel is additionally hot-rolled to produce hot-rolled steel.

Product name	Activity name	Region	Annual production volume (source: ecoinvent) [kg]	Correction for reinforcing steel using unalloyed and low-alloyed steel + share of hot rolling [kg]	Production share
steel, chromium steel 18/8	market for steel, chromium steel 18/8	GLO	5.22E+10	2.61E+10	1.8%
steel, chromium steel 18/8, hot-rolled	market for steel, chromium steel 18/8, hot-rolled	GLO	2.61E+10	2.61E+10	1.8%
steel, low-alloyed	market for steel, low-alloyed	GLO	1.53E+11	5.29E+10	3.7%
steel, low-alloyed, hot-rolled	market for steel, low-alloyed, hot-rolled	GLO	7.65E+10	7.65E+10	5.3%
steel, unalloyed	market for steel, unalloyed	GLO	1.23E+12	1.19E+12	82.9%
reinforcing steel	market for reinforcing steel	GLO	6.39E+10	6.39E+10	4.5%
Total			1.50E+12	1.44E+12	100%

1.4.4. Alloying elements

Low-alloyed steel

BOF-based low-alloyed steelmaking:

Primary production routes are based on the BOF process from ecoinvent, i.e. “steel production, converter, low-alloyed, RER”, and therefore already consider alloying elements.

Scrap-EAF low-alloyed steelmaking:

Scrap-EAF is based on the process from ecoinvent (“steel production, electric, low-alloyed”), which already accounts for alloying elements (FeMn, FeSi).

EAF-based low-alloyed primary steelmaking:

The original alloying elements of FeMn and FeSi from the ecoinvent process for scrap-EAF steelmaking are set to zero. Instead, the alloying elements to produce low-alloyed steel were assumed as in the ecoinvent process to produce 1 kg low-alloyed steel with a converter (BOF), i.e. “steel production, converter, low-alloyed, RER”. These are the following three elements:

- ferromanganese (FeMn): controls the amount of carbon in the steel and deoxidizing agent (e.g. to avoid blowholes caused by oxygen during cooling of the steel)
- ferronickel (FeNi): increases heat-resistance
- molybdenite (Mb): for high strength and corrosion-resistant steel

These alloys are added to all EAFs used for low-alloyed steelmaking in new primary production routes (H2-DRI, EW, NG-DRI, NG-DRI+CCS).

This assumes that these alloying elements are usually already present in the scrap entering a scrap-EAF, which is not the case here, where low-alloyed steel is produced from primary iron. To make the primary production routes comparable, the same alloying elements are assumed for all primary steelmaking technologies.

Unalloyed steel

BOF-based unalloyed steelmaking:

Primary production routes are based on the BOF process from ecoinvent, i.e. “steel production, converter, unalloyed, RER”, and therefore already consider the input of ferromanganese (FeMn).

Scrap-EAF unalloyed steelmaking:

Due to a lack of data, we assume the same process for scrap-EAF unalloyed steelmaking as for low-alloyed steelmaking which is based on the original ecoinvent process (“steel production, electric, low-alloyed”).

If the respective input material (scrap, high-quality scrap, etc.) is managed accordingly, all kinds of steel can be produced from the EAF³⁶. For the future, we assume that advanced sorting technologies will enable the required control of input material to allow the production of all steel grades from the EAF.

EAF-based unalloyed primary steelmaking:

The same reasoning applies as for low-alloyed steel. The original alloying elements of FeMn and FeSi from the ecoinvent process for scrap-EAF steelmaking are set to zero. Instead, the alloying elements to produce low-alloyed steel were assumed as in the ecoinvent process to produce 1 kg unalloyed steel with a converter (BOF), i.e. “steel production, converter, unalloyed, RER”, which is ferromanganese (FeMn).

This applies to all EAFs used for unalloyed steelmaking in new primary production routes (H2-DRI, EW, NG-DRI, NG-DRI+CCS). The amount of ferromanganese for unalloyed steel from the BOF is about 60% lower than for low-alloyed steel from the BOF and about 40% lower than for low-alloyed steel from the scrap-EAF in ecoinvent.

Other steel types

Alloying elements of other steel types (chromium and reinforced) are not changed but assumed as in ecoinvent, since the new primary production routes are not directly incorporated for these steel types. However, reinforcing steel is produced from low-alloyed and unalloyed steel (Figure S15) and therefore indirectly influenced by the assumptions for them.

1.4.5. Distinction between primary and secondary steel production

To align the assumptions in the IMAGE scenarios with our LCA model, we adapt the LCA model (this modification is discussed in section 3.2.1). The IMAGE model distinguishes between primary and secondary steel production pathways and production amounts. For consistency reasons, the LCA model applies the same distinction of primary and secondary routes. This affects both input material, e.g. primary or secondary iron, as well as waste streams, e.g. BOF slag or secondary BOF slag.

Input material:

In ecoinvent, primary production routes (BOF) partly receive iron scrap, i.e. a secondary material, while secondary production processes (scrap-EAF) partly receive primary material input, e.g. sponge iron and pig iron, in specific regions (RoW, India).

The BOF datasets should be purely based on primary inputs, while the EAF datasets should be purely scrap-based. Hence, we set the respective input of scrap (for BOFs) or primary iron (for scrap-EAF) to zero and add their amounts to the respective primary input (for BOFs) or to secondary input (for scrap-EAF). The resulting modifications of BOF and EAF datasets are also listed in Table S5.

Waste flows:

The same principle is applied to the slag streams (see Table S5).

1.5. Impact assessment methods

Table S8: Additional characterization factors (CFs) for biogenic carbon flows and hydrogen emissions to air ³⁷ are implemented in addition to the CFs for GWP of the IPCC 2013 100a method. Source: ³².

Elemental flow	Category	Amount (CO ₂ -eq)	Unit
Carbon dioxide, in air	('natural resource', 'in air')	-1	kg
Carbon dioxide, non-fossil, resource correction	('natural resource', 'in air')	-1	kg
Carbon dioxide, non-fossil	('air', 'lower stratosphere + upper troposphere')	1	kg
Carbon dioxide, non-fossil	('air',)	1	kg
Carbon dioxide, non-fossil	('air', 'urban air close to ground')	1	kg
Hydrogen	('air', 'low population density, long-term')	11	kg
Hydrogen	('air', 'lower stratosphere + upper troposphere')	11	kg
Hydrogen	('air', 'non-urban air or from high stacks')	11	kg
Hydrogen	('air',)	11	kg
Hydrogen	('air', 'urban air close to ground')	11	kg

Table S9: Applied impact categories and impact assessment methods. Source: ³²

Environmental impact category	Impact assess. family	Environmental impact assessment method	CF Unit
Climate Change	IPCC 2021	IPCC 2021 GWP 100a + additional CFs from Table S8	kg CO ₂ -eq
Ecotoxicity: freshwater	EF v3.0	comparative toxic unit for ecosystems (CTU _e)	CTU _e
Energy resources: non-renewable	EF v3.0	abiotic depletion potential (ADP): fossil fuels	MJ, net calorific value
Eutrophication: freshwater	EF v3.0	fraction of nutrients reaching freshwater end compartment (P)	kg PO ₄ -Eq
Eutrophication: marine	EF v3.0	fraction of nutrients reaching marine end compartment (N)	kg N-Eq
Eutrophication: terrestrial	EF v3.0	accumulated exceedance (AE)	mol N-Eq
Human toxicity: carcinogenic	EF v3.0	comparative toxic unit for human (CTU _h)	CTU _h
Human toxicity: non-carcinogenic	EF v3.0	comparative toxic unit for human (CTU _h)	CTU _h
Ionising radiation: human health	EF v3.0	human exposure efficiency relative to u235	kBq U ₂₃₅ -Eq
Land use	EF v3.0	soil quality index	dimensionless
Material resources: metals/minerals	EF v3.0	abiotic depletion potential (ADP): elements (ultimate reserves)	kg Sb-Eq
Ozone depletion	EF v3.0	ozone depletion potential (ODP)	kg CFC-11-Eq
Particulate matter formation	EF v3.0	impact on human health	disease incidence
Photochemical ozone formation: human health	EF v3.0	tropospheric ozone concentration increase	kg NMVOC-Eq
Water use	EF v3.0	user deprivation potential (deprivation-weighted water consumption)	m ³ world eq. deprived

2 Results

2.1. Impacts of iron ore pellets and iron sinter production

Depending on the iron production technology, the iron-bearing raw material can be iron sinter, iron ore pellets, iron ore concentrates, iron oxides or a mix of several of them (see Table S10).

Table S10: Inputs of iron-bearing materials per primary production route.

Production route(s)	Iron-bearing input materials in kg/kg iron produced	Sum of iron-bearing materials in kg/kg steel unalloyed
BF-BOF, BF-BOF-CCS, TGR-BF-BOF, TGR-BF-BOF-CCS	1.05 kg iron sinter/kg iron + 0.4 kg pellets/kg iron	1.6 kg iron sinter and pellets
NG-DRI- EAF, NG-DRI- EAF-CCS	1.375 kg iron ore pellets/kg NG-DRI iron	1.46 kg iron ore pellets
H2-DRI-EAF	1.36 kg iron ore pellets / kg H2- DRI	1.44 kg iron ore pellets
EW-EAF	1.46 kg iron ore oxides	1.55 kg iron ore oxides

The specific climate change impacts of iron pellet production are 80% lower than those of iron sinter production based on datasets from ecoinvent 3.9.1 (see Figure S16). Thus, the contribution of the raw materials of iron sinter compared to iron pellets to the specific impact per steel production route can differ considerably.

The relatively high contribution of direct emissions of iron sinter plants to steelmaking aligns with previous research^{38,39}. Besides their high greenhouse gas emissions, they are a major source of dust (particulate matter) as well as respective precursors, such as NO_x or SO₂, which drive human health impacts at the local level^{38,39}.

	Climate change impact		Process contribution	
	kg CO ₂ eq./kg product		%	
	Iron pellet	Iron sinter	Iron pellet	Iron sinter
Total	0.099	0.504	100%	100%
diesel, burned in building machine	0.006		6%	0%
electricity production, hard coal	0.021	0.025	21%	5%
electricity production, lignite	0.004		4%	0%
hard coal mine operation and hard coal preparation	0.008	0.016	8%	3%
iron pellet production	0.025		25%	0%
iron sinter production		0.321	0%	64%
quicklime production, in pieces, loose		0.034	0%	7%
transport, freight, sea, bulk carrier for dry goods		0.028	0%	6%
Rest	0.036	0.079	36%	16%

Figure S16: Climate change impacts of producing 1 kg of iron ore pellets and iron ore sinter. Functional units: 1) iron pellet production, RoW, ecoinvent 3.9.1 (cutoff) 2) iron sinter production, RoW, ecoinvent 3.9.1 (cutoff). Process contributions for top 5 contributors, aggregated by process name.

2.2. Specific impacts of steel and electricity markets

2.2.1. Steel markets

While the impact trends in the 3.5°C scenario are mostly minor and primarily decreasing in all impact categories, impacts gradually intensify in the 2°C and 1.5°C scenario, exhibiting the greatest changes in the 1.5°C scenario.

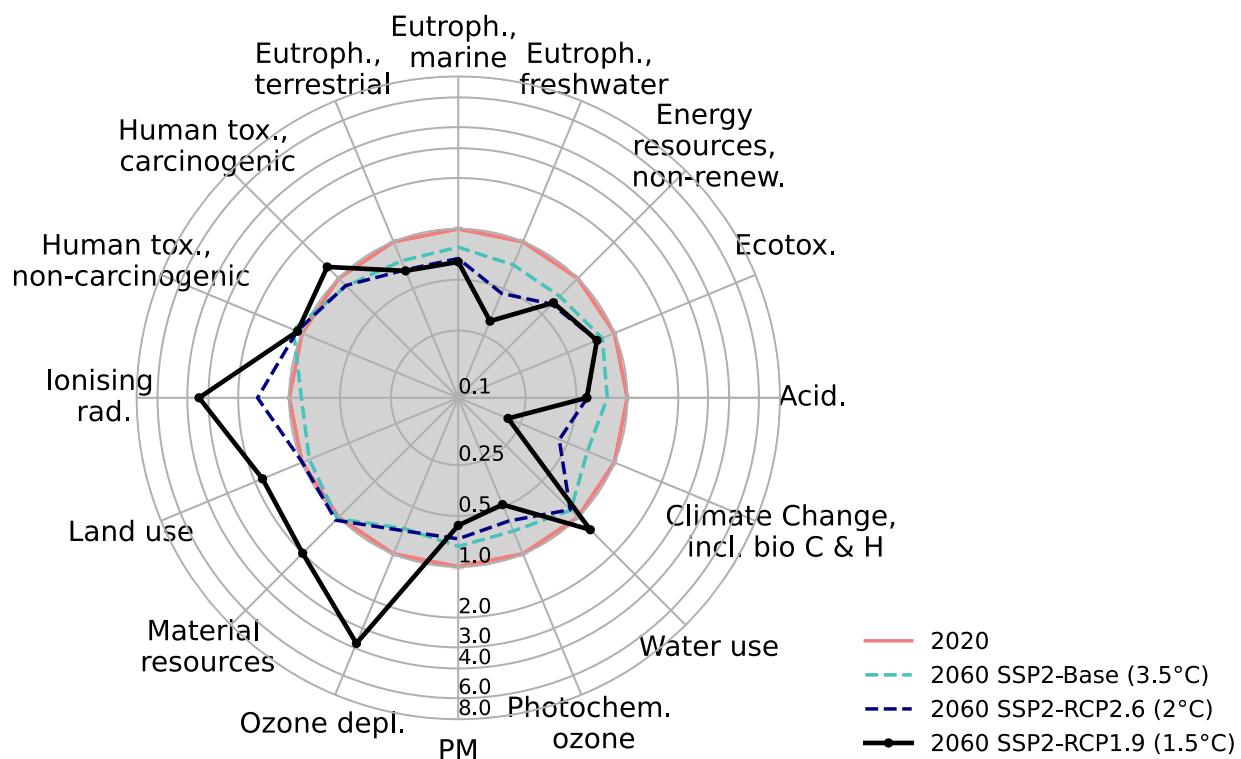
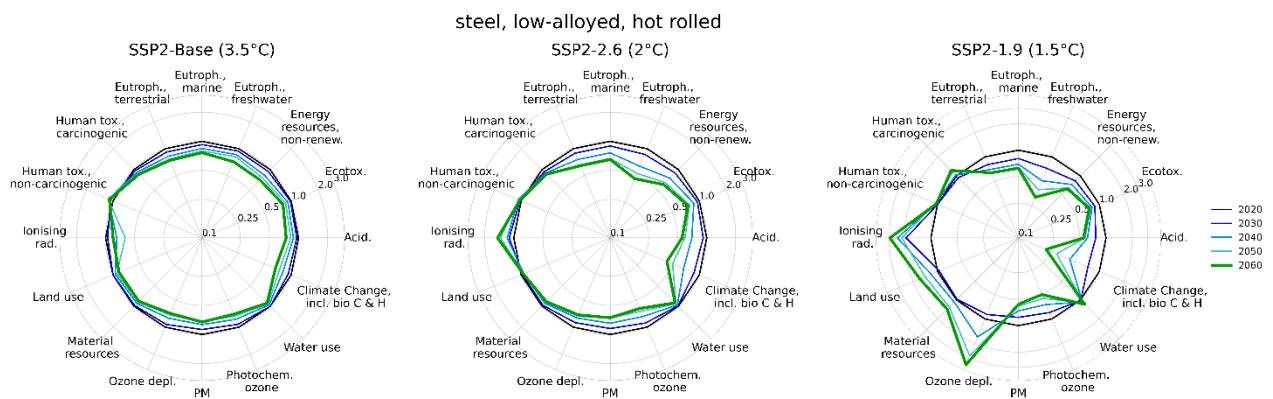
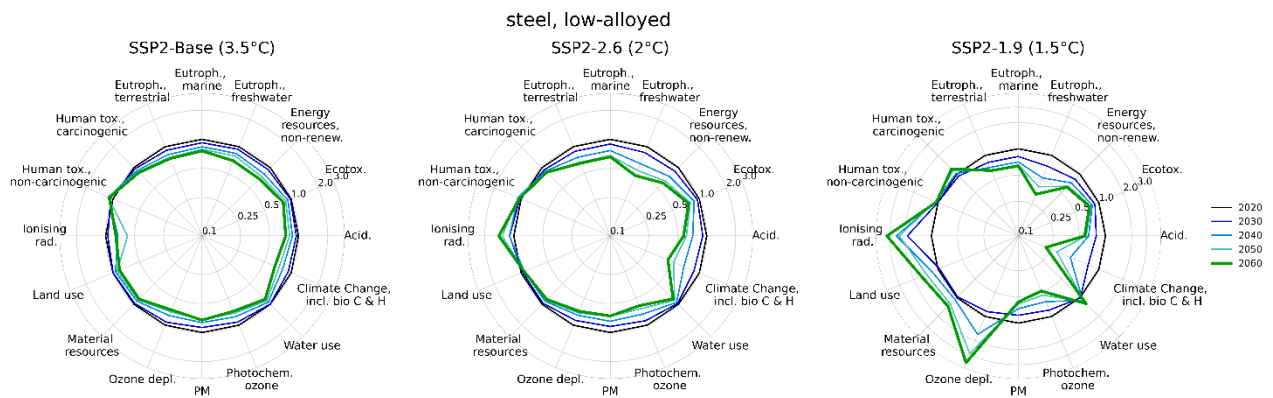
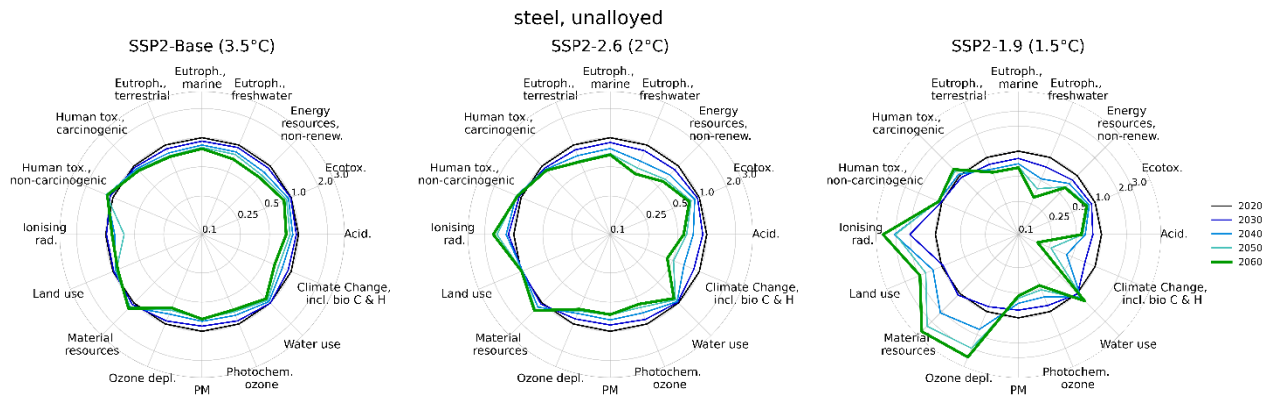
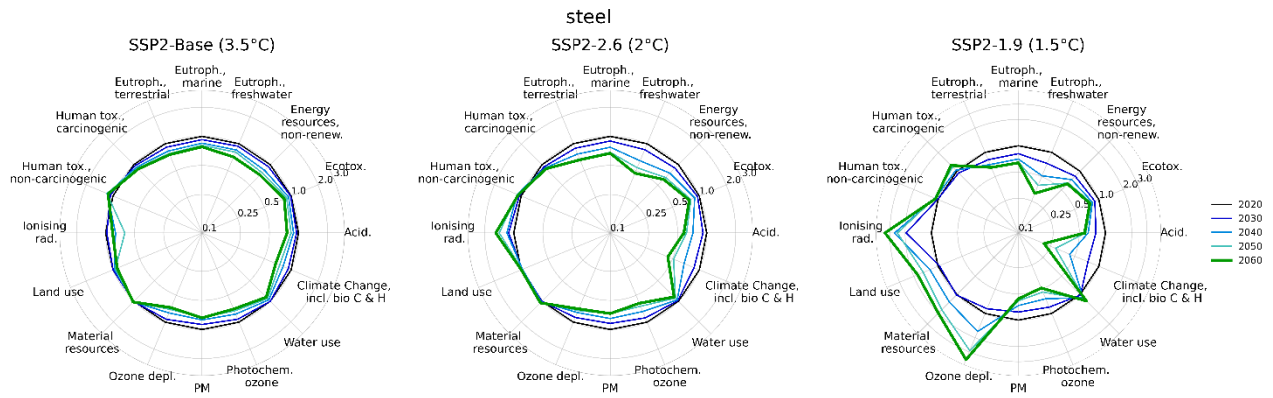


Figure S17: Impact development of steel production in 2060 compared to 2020 for impacts per kg steel. Values are relative to the impacts in 2020 on a logarithmic scale. Functional unit: 1 kg steel from the global market for steel; premise: all background scenarios are incorporated. Acid.: acidification; Ecotox.: ecotoxicity; Energy res., non-renew.: non-renewable energy resources; Eutroph., freshwater: freshwater eutrophication; Eutroph., marine: marine eutrophication; Eutroph., terrestrial: terrestrial eutrophication; Human tox., carc.: carcinogenic human toxicity; Human tox., non-carc.: non-carcinogenic human toxicity; Ionising rad.: ionising radiation; Ozone depl.: ozone depletion; PM: particulate matter; Photochem. ozone: photochemical ozone formation; incl. bio C & H: including biogenic carbon and hydrogen.



2.2.2. Electricity markets

Figure S19 illustrates the impacts of electricity generation in 2060 compared to 2020 for all scenarios per kWh of electricity generated. It shows that impacts increase for ionising radiation, land use, material resources, and ozone depletion.

The impacts of ionising radiation are caused by processes related to nuclear power (i.e., uranium mining, related mining waste and the reprocessing of spent nuclear fuel). As such, the trend of ionising radiation depends on the scenario and it coincides with the shares of nuclear power in the assumed electricity mix (see section 1.2.5), which is the lowest in the Base scenario (7%), and the highest in the 2°C scenario, i.e., 12% of power generation in 2060. Thus, these adverse side effects may be reduced under a different electricity mix, excluding nuclear power.

Material resource depletion impacts increase due to higher requirements for tellurium, copper, gold, and silver (Figure S20). These metals are required for more electrified and renewable power systems, e.g., PV panels and wind turbines. Solar and wind energy are expected to have higher shares of power generation in the IMAGE 1.5°C scenario (Figure S10).

Impact category	Scenario	Impacts in 2060 relative to 2020
Climate change	SSP2-Base	-31%
	SSP2-RCP2.6	-104%
	SSP2-RCP1.9	-108%
Acidification	SSP2-Base	-28%
	SSP2-RCP2.6	-91%
	SSP2-RCP1.9	-92%
Ecotoxicity	SSP2-Base	-38%
	SSP2-RCP2.6	-80%
	SSP2-RCP1.9	-82%
Non-renewable energy resources	SSP2-Base	-26%
	SSP2-RCP2.6	-57%
	SSP2-RCP1.9	-66%
Freshwater eutrophication	SSP2-Base	-22%
	SSP2-RCP2.6	-93%
	SSP2-RCP1.9	-97%
Marine eutrophication	SSP2-Base	-33%
	SSP2-RCP2.6	-82%
	SSP2-RCP1.9	-84%
Terrestrial eutrophication	SSP2-Base	-35%
	SSP2-RCP2.6	-77%
	SSP2-RCP1.9	-78%
Carcinogenic human toxicity	SSP2-Base	-23%
	SSP2-RCP2.6	-48%
	SSP2-RCP1.9	-36%
Non-carcinogenic human toxicity	SSP2-Base	-29%
	SSP2-RCP2.6	-69%
	SSP2-RCP1.9	-68%
Ionising radiation	SSP2-Base	-19%
	SSP2-RCP2.6	35%
	SSP2-RCP1.9	4%
Land use	SSP2-Base	1%
	SSP2-RCP2.6	24%
	SSP2-RCP1.9	58%
Material resources	SSP2-Base	24%
	SSP2-RCP2.6	66%
	SSP2-RCP1.9	84%
Ozone depletion	SSP2-Base	20%
	SSP2-RCP2.6	41%
	SSP2-RCP1.9	56%
Particulate matter formation	SSP2-Base	-52%
	SSP2-RCP2.6	-81%
	SSP2-RCP1.9	-82%
Photochemical oxidant formation	SSP2-Base	-30%
	SSP2-RCP2.6	-76%
	SSP2-RCP1.9	-79%
Water use	SSP2-Base	-26%
	SSP2-RCP2.6	-23%
	SSP2-RCP1.9	-30%

Figure S19: Impact development by 2060 relative to 2020 for electricity generation. Functional unit: 1 kWh from the market group for electricity, medium voltage (Region=World); premise: all background scenarios are incorporated.

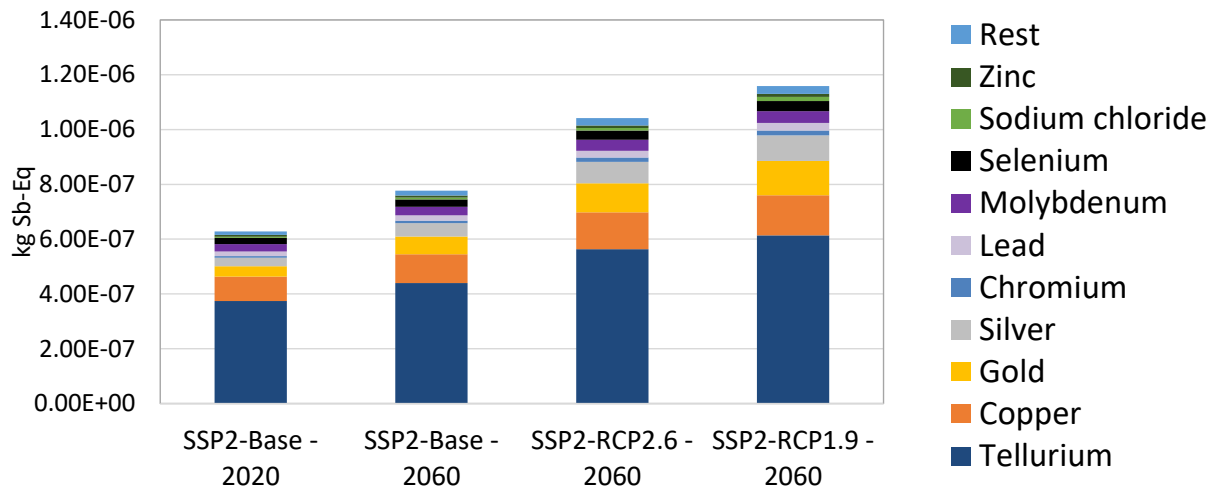


Figure S20: Contribution analysis for material resource depletion impacts per kWh electricity. Functional unit: 1 kWh from the market group for electricity, medium voltage (Region=World); premise: all background scenarios are incorporated. Elementary flow contributions showing top 10 contributors in each year, aggregated by name.

2.3. Contribution analysis for specific impacts of global steel production

The underlying data for the contribution analysis presented in Figure 8 is provided in the table below.

Table S11: Contribution analysis of impacts per kg steel for 16 impact categories showing the top five contributing processes aggregated by process name (underlying data for Figure 8). Functional unit: 1 kg of steel from the global market group for steel, premise: all background scenarios are incorporated.

	2020	SSP2-Base 2060	SSP2-RCP2.6 2060	SSP2-RCP1.9 2060
Acidification				
blasting			7%	6%
coking	8%		7%	
electricity production, hard coal	8%	8%		
electricity production, lignite	7%	8%		
heat production, at hard coal industrial furnace 1-10MW		8%	10%	11%
iron sinter production	11%	11%	12%	
platinum group metal mine operation, ore with high palladium content				5%
smelting of copper concentrate, sulfide ore				9%
transport, freight, sea, bulk carrier for dry goods	15%	14%	16%	16%
Ecotoxicity				
blasting	45%	40%	39%	37%
hard coal mine operation and hard coal preparation	27%	15%	11%	5%
heat production, at hard coal industrial furnace 1-10MW	2%		2%	2%
market for wastewater, average	15%	30%	34%	36%
treatment of drilling waste, landfarming		2%	3%	4%
treatment of water discharge from petroleum/natural gas extraction, onshore	2%	2%		
Energy resources				
hard coal mine operation	4%	4%		
hard coal mine operation and hard coal preparation	61%	49%	40%	17%
lignite mine operation	2%	3%		

	2020	SSP2-Base 2060	SSP2-RCP2.6 2060	SSP2-RCP1.9 2060
petroleum and gas production, offshore	8%	11%	13%	20%
petroleum and gas production, onshore	17%	23%	27%	34%
uranium mine operation, underground			5%	10%
uranium production, in yellowcake, in-situ leaching			4%	8%
Eutrophication, freshwater				
market for wastewater, average	2%	6%	9%	14%
treatment of basic oxygen furnace slag, residual material landfill	17%	13%	17%	9%
treatment of electric arc furnace slag, residual material landfill				8%
treatment of spoil from hard coal mining, in surface landfill	61%	53%	59%	39%
treatment of spoil from lignite mining, in surface landfill	14%	19%	3%	
treatment of sulfidic tailings, from copper mine operation, tailings impoundment	2%	3%	5%	17%
Eutrophication, marine				
blasting	9%	8%	9%	9%
diesel, burned in building machine	6%	8%	9%	10%
iron sinter production	10%	9%	9%	
transport, freight train, diesel	7%	7%		7%
transport, freight, sea, bulk carrier for dry goods	16%	15%	15%	16%
treatment of wastewater, average, wastewater treatment			8%	9%
Eutrophication, terrestrial				
blasting	14%	14%	14%	13%
diesel, burned in building machine	7%	8%	9%	10%
heat production, at hard coal industrial furnace 1-10MW				5%
iron sinter production	11%	10%	10%	
transport, freight train, diesel	8%	8%	8%	7%
transport, freight, sea, bulk carrier for dry goods	18%	16%	16%	17%
Human toxicity, carcinogenic				
coking	45%	30%	24%	6%
steel production, electric, low-alloyed	1%	2%	2%	1%
treatment of basic oxygen furnace slag, residual material landfill	5%	3%	3%	1%
treatment of electric arc furnace dust, residual material landfill	1%	1%	1%	2%
treatment of electric arc furnace slag, residual material landfill	45%	61%	67%	88%
Human toxicity, non-carcinogenic				
coking	7%	3%	3%	
ferronickel production	4%	3%	3%	4%
iron sinter production	26%	17%	16%	5%
market for wastewater, average	18%	27%	29%	31%
smelting of copper concentrate, sulfide ore				7%
steel production, electric, low-alloyed	21%	32%	32%	32%
Ionising radiation				
electricity production, nuclear, boiling water reactor	10%	13%	10%	11%
electricity production, nuclear, pressure water reactor	5%	4%	5%	5%
treatment of low level radioactive waste, plasma torch incineration	5%	5%	5%	5%
treatment of spent nuclear fuel, reprocessing	15%	21%	20%	22%

	2020	SSP2-Base 2060	SSP2-RCP2.6 2060	SSP2-RCP1.9 2060
treatment of tailing, from uranium milling	62%	55%	58%	56%
Land Use				
hard coal mine operation and hard coal preparation	21%	13%	8%	
hardwood forestry, beech, sustainable forest management	8%			
hardwood forestry, birch, sustainable forest management		7%	10%	15%
open ground construction, on ground				12%
railway track construction	5%			
residual material landfill construction	6%			
road construction	16%	16%	13%	9%
softwood forestry, pine, sustainable forest management		7%	11%	16%
softwood forestry, spruce, sustainable forest management		7%	11%	17%
Material resources				
chromite ore concentrate production	40%	40%	39%	21%
cobalt production	6%	7%	6%	4%
copper mine operation and beneficiation, sulfide ore	35%	34%	35%	43%
ferronickel production	5%	5%	5%	
sodium chloride production, powder				12%
zinc mine operation	4%	4%	3%	3%
Ozone depletion				
chlor-alkali electrolysis, diaphragm cell	1%		3%	15%
chlor-alkali electrolysis, membrane cell	3%	4%	12%	66%
chlor-alkali electrolysis, mercury cell				4%
coking	76%	64%	50%	3%
petroleum and gas production, offshore	17%	25%	26%	7%
purified terephthalic acid production		1%		
transport, pipeline, onshore, long distance, natural gas	1%	1%		
trichloromethane production			2%	
Particulate matter				
diesel, burned in building machine		5%		7%
electricity production, hard coal, at coal mine power plant	32%	20%	15%	8%
ferrosilicon production	5%	15%	16%	20%
heat production, at hard coal industrial furnace 1-10MW	4%		5%	7%
iron pellet production	4%	5%	6%	
iron sinter production	17%	17%	16%	6%
Photochemical ozone formation				
blasting	5%	5%	5%	6%
coking	35%	29%	27%	12%
diesel, burned in building machine				7%
iron sinter production	13%	13%	14%	
natural gas venting from petroleum/natural gas production	5%	6%	8%	13%
transport, freight, sea, bulk carrier for dry goods	9%	9%	9%	11%
Water use				
BF-BOF, steel production, unalloyed [CH]	27%	13%	7%	
air separation, cryogenic	11%	13%	12%	

	2020	SSP2-Base 2060	SSP2-RCP2.6 2060	SSP2-RCP1.9 2060
chlor-alkali electrolysis, diaphragm cell				8%
chlor-alkali electrolysis, membrane cell				12%
electricity production, hydro, reservoir, alpine region	8%	8%	9%	9%
electricity production, nuclear, pressure water reactor, heavy water moderated				8%
hot rolling, steel		6%		
iron pellet production			8%	
steel production, electric, low-alloyed	11%	21%	20%	14%
hard coal mine operation and hard coal preparation	6%			
Climate change				
TGR-BF+CCS, iron production [CH]				18%
TGR-BF, iron production [CH]		6%	10%	
coking	4%			
electricity production, at co-generation natural gas-fired power plant, post, pipeline 200km, storage 1000m				-16%
electricity production, hard coal	11%	9%		
hard coal mine operation and hard coal preparation	8%	6%	7%	
heat and power co-generation, natural gas, conventional power plant, 100MW electrical				21%
heat production, at hard coal industrial furnace 1-10MW			6%	14%
iron sinter production	13%	13%	17%	
pig iron production	31%	18%	15%	
supply of forest residue				-26%

2.3.1. Human toxicity (carcinogenic)

The impacts of carcinogenic human toxicity increase in the global market group for steel by up to +25% (RCP 1.9 in 2060). The main contributor is the process of “treatment of electric arc furnace slag, residual material landfill” which is responsible for 88% of the impacts in 2060 and occurs in steel making processes with the EAF. The main emission during the process of landfill is chromium VI to surface water, causing 91% of impacts of carcinogenic human toxicity (RCP 1.9 in 2060).

For the BF-BOF route, the driving process is the coke production (i.e. “coking”) and its emission of Benzo(a)pyrene to air, which causes 73% of carcinogenic human toxicity impacts of unalloyed BF-BOF steel. The human toxicity impacts of the scrap-EAF route are about 42% higher than those of the BF-BOF route.

In the RCP1.9 scenario, the main primary production technologies depend on the EAF for steel making (e.g., EW-EAF, NG-DRI-EAF). Since the human toxicity impacts of the EAF routes are higher than for the BOF routes, these impacts increase in scenarios with a high share of the EAF.

However, this increase in human toxicity impacts might be overestimated for the following reasons. First, the emissions from outflows of the EAF are highly dependent on the input material into the furnace. Currently, the EAF in ecoinvent 3.9.1 is modelled based on the assumptions that it primarily consumes scrap (old and new scrap)⁴⁰, which may be contaminated and may contain a mix of alloys. In the future, with the EAF being used for primary production as well, e.g. for electrowinning, the inflows of the EAF will be less contaminated. Secondly, new policies aim to reduce landfills in the future, which will also reduce corresponding emissions from landfills.

2.3.2. Ionising radiation

The main cause of ionising radiation impacts is nuclear power generation. By 2060, under the 1.5°C scenario, the main contributors are:

- the treatment of tailings from uranium milling (56%), which releases Radon-222 to the air;
- the treatment and reprocessing of spent nuclear fuel (22%), which is one of several sources of carbon isotope emissions to the air (i.e., carbon-14);
- and lastly, the process of nuclear electricity production with boiling water reactors (7%), which releases carbon isotopes in the cooling system.

The main emissions are radon-222 and carbon-14, which contribute 56% and 41%, respectively, thus representing 97% of emissions.

The increase in ionising radiation is due to an increased power demand for the much more electrified steel production by 2060 under the 1.5°C scenario. It strongly depends on the electricity mix, which in this scenario includes nuclear power (9%, see section 1.2.5).

2.3.3. Material resource depletion

Although the impacts of material resource depletion grow by 100% by 2060 in the 1.5°C scenario, they stay about constant in the other two scenarios, exhibiting an increase of only 3% and 6% in the Base and 2°C scenarios, respectively, as illustrated in Figure S21. This strong increase in the 1.5°C scenario is primarily driven by higher contributions from tellurium, copper, gold and silver, and sodium chloride.

Metals like tellurium, copper, gold and silver are required for low-carbon technologies, like PV panels (e.g., cadmium telluride thin-film PV) or wind turbines, needed for renewable power generation and electrified systems in general, e.g., due to their high conductivity. As shown in Figure S20, material resource depletion of power generation increases considerably in the 1.5°C scenario, driven by the same metals as for the steel market. Tellurium and gold have very high depletion potential (characterisation factors) in the impact assessment method used.

Steel production's electricity requirements will increase by 2060 due to more electrified steel production via EW and scrap-EAF, which will have higher market shares in 2060 than in 2020. Sodium chloride is needed to produce sodium hydroxide, the electrolyte required for EW.

Chromium for chromium steel has a high contribution (21-40%, depending on the scenario). Still, its impact remains almost constant, as its production share per kg of steel from the global market is assumed to be constant.

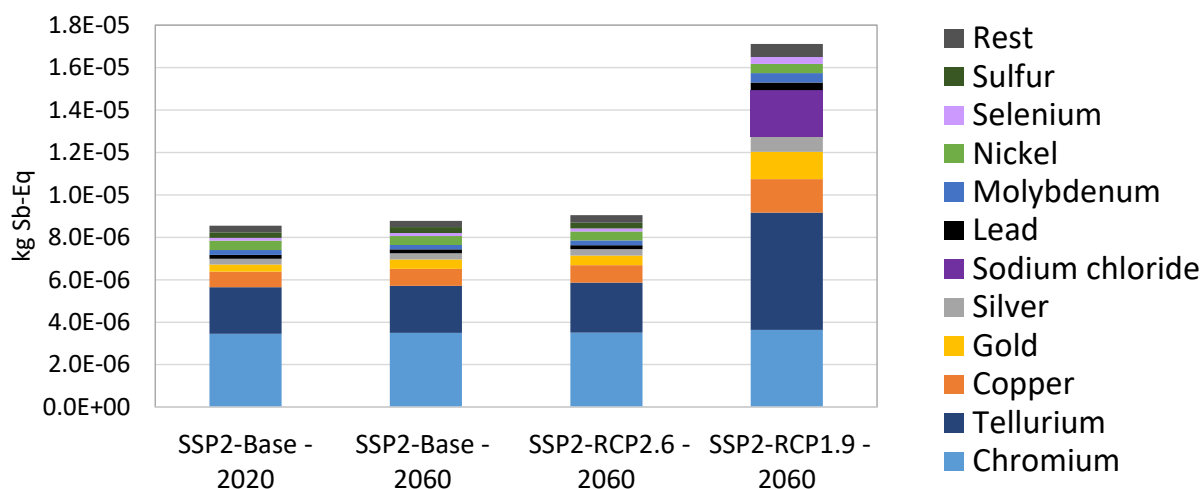


Figure S21: Contribution analysis for material resource depletion impacts per kg steel from the global market of steel. Functional unit: 1 kg steel from the global market group for steel; premise: all background scenarios are incorporated. Elementary flow contributions showing top 10 contributors, which are aggregated by name.

2.3.4. Ozone depletion

Assessments of current and future ozone depletion impacts are subject to very high uncertainty and are likely overestimated, as ozone-depleting substances are being phased out due to the Montreal Protocol, which was adopted in 1989. Consumption of ozone-depleting substances to date has fallen below 1% of historical peak values in 1989⁴¹. This phase-out is, however, neither sufficiently represented in current life-cycle inventory databases, like ecoinvent, nor in futurized databases based on ecoinvent⁴². As such, ozone depletion impacts are inherently overestimated, which has already been emphasized by prior studies⁴².

Despite this high uncertainty, we present our results for ozone depletion impacts for the sake of complete transparency below and due to the lack of better data.

In 2020, ozone depletion is dominated by coke production, which causes 76% of impacts. In the Base and 2°C scenarios, ozone depletion impacts decrease by about 30% due to lower coke requirements. In the 1.5°C scenario, they may rise driven by the production of sodium hydroxide, which reaches a contribution of 84% by 2060. Sodium hydroxide is the alkaline electrolyte required for EW. It is produced via chlor-alkali electrolysis, mostly using membrane cells, which releases tetrachloromethane according to the datasets defined in ecoinvent v3.9. Emissions of tetrachloromethane, also called carbon tetrachloride, cause about 86% of ozone depletion impacts in 2060 under the 1.5°C scenario. However, current consumption of carbon tetrachloride is approaching very low levels⁴¹. Hence, these rising impacts are likely overestimated and are probably an artefact of datasets from ecoinvent.

2.4. Specific impacts under varying background scenarios

The benefit of ambitious electrified steel scenarios becomes effective only if the electricity sector is decarbonized. Solely electrifying steel production, as in the 1.5°C scenario, cannot reduce climate change impacts. Only in combination with decarbonizing electricity can the impacts of steel production decrease by 79% by 2060 (Figure S22).

In most impact categories, realizing the climate-ambitious steel scenarios alone even increases impacts compared to the conservative 3.5°C scenario (Figure S22). Exceptions are particulate matter and photochemical ozone formation, as they co-benefit from the phase-out of coal-based steel production processes (section 3.3.1).

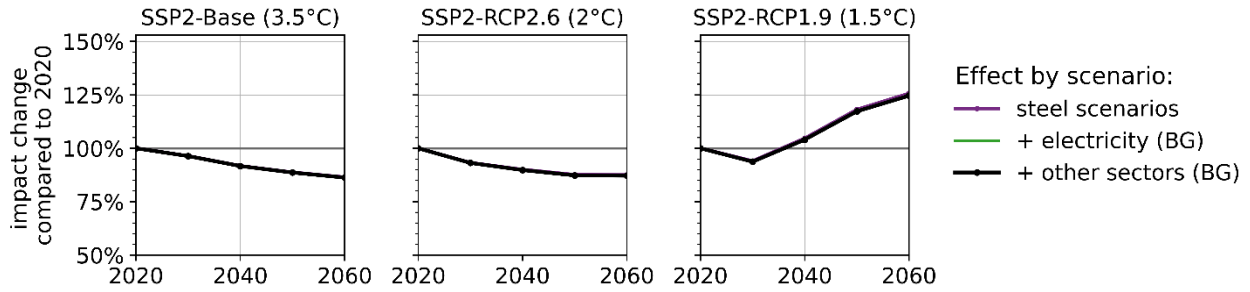
Adding more BG scenarios, e.g., for electricity, can only partly, but not entirely, compensate for these growing impacts due to the steel scenario. For instance, carcinogenic human toxicity is only driven by steel production processes, specifically coke production and the treatment of EAF slag (section 2.3). There is an exception for ionising radiation, land use and material resources, where the background electricity scenarios even further intensify future impacts of steel (see section 3.3.1). Hence, improvements along the entire supply chain with process- and impact-category-specific measures are required.

Thus, drastically decarbonizing the steel sector requires more renewable upstream supply processes to avoid unwanted side-effects, i.e. increasing instead of decreasing impacts, or of a lower impact reduction in the 1.5°C scenario than in the 3.5°C or 2°C scenario (see e.g. climate change, photochemical ozone formation, or particulate matter). The fact that the 1.5°C scenario performs worse than the 2°C scenario if only the steel sector is decarbonized applies to all impact categories, including those where impact trends are expected to decrease overall (Figure S22.b).

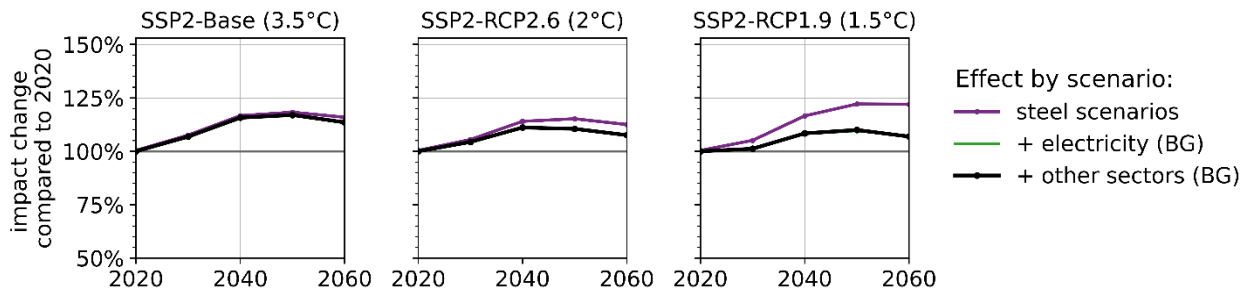
Among all the background scenarios investigated in this study, the major driver of impact reduction is the electricity supply (green line), as the additional background scenarios barely affect the final impact trend (black line, which mostly coincides with the green line). The reason for this is that the energy input of electricity gains in relevance, as the shares of the electricity-based steel production technologies increase globally: secondary production increases from 21% to 39%; and for primary production EW-EAF supplies up to 30% of steel in the 1.5°C scenario.

a) Overall increasing impacts

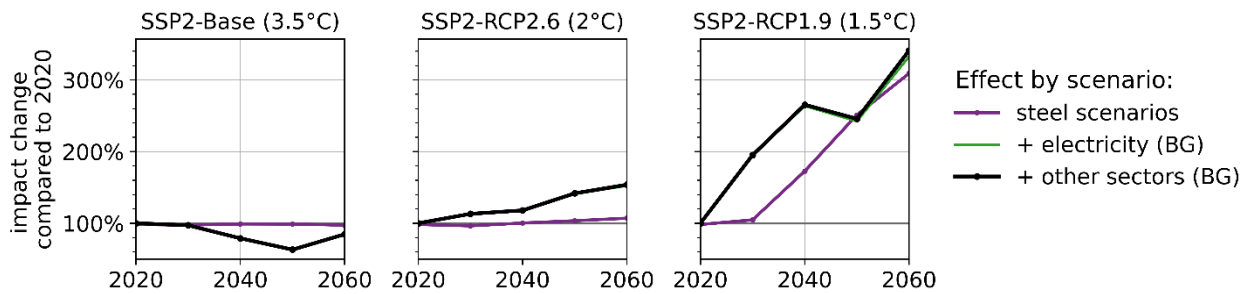
Human toxicity, carcinogenic



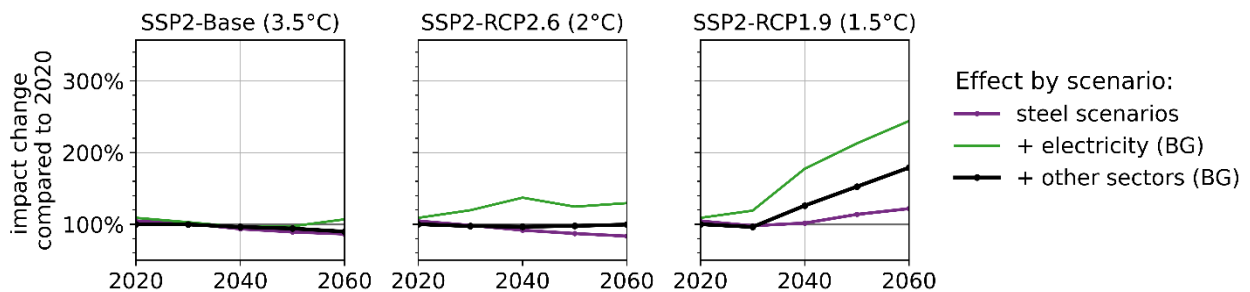
Human toxicity, non-carcinogenic



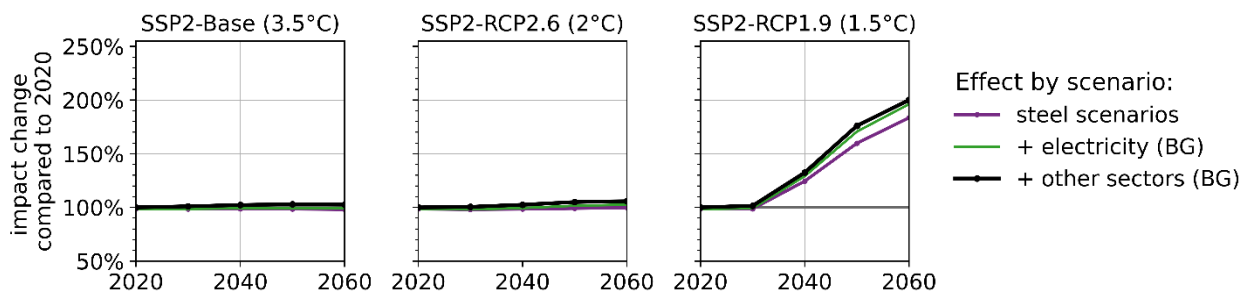
Ionising radiation



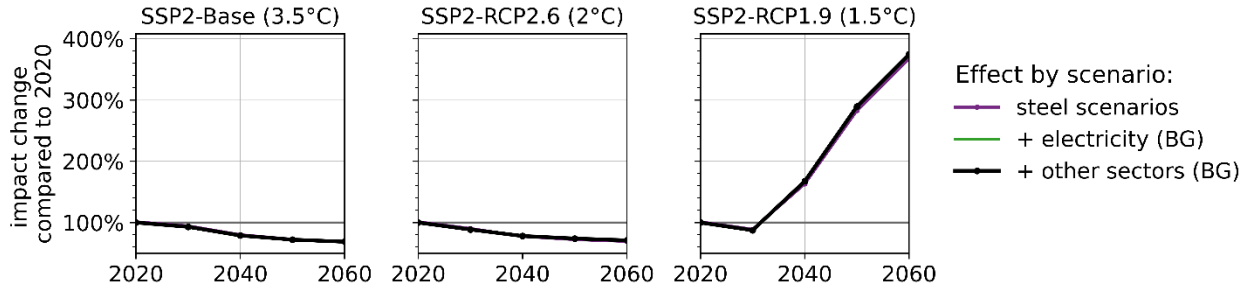
Land use



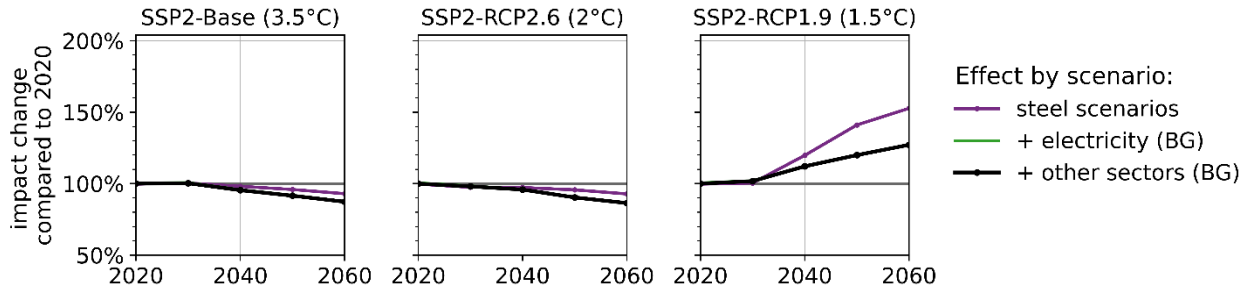
Material resources, metal and minerals



Ozone depletion

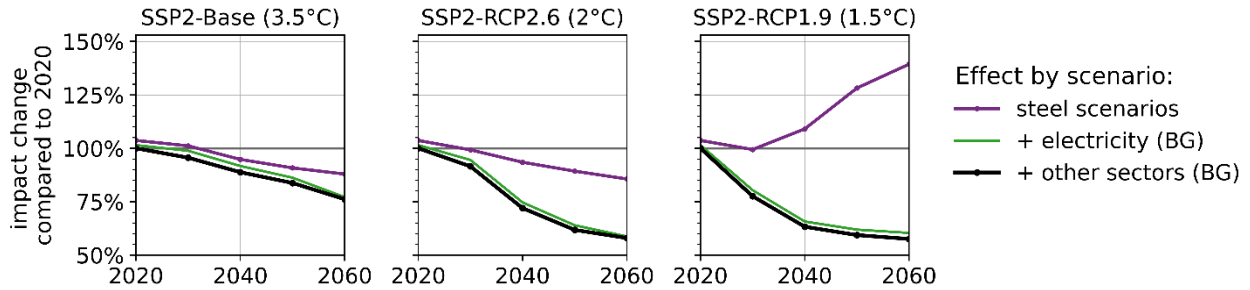


Water use

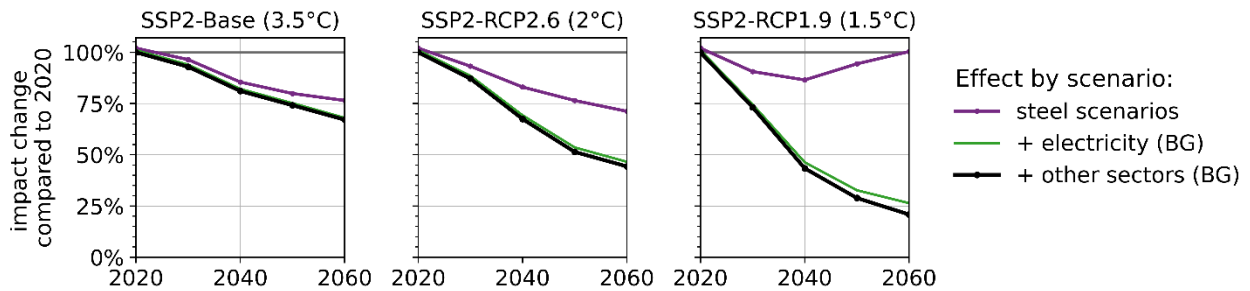


b) Overall decreasing impacts

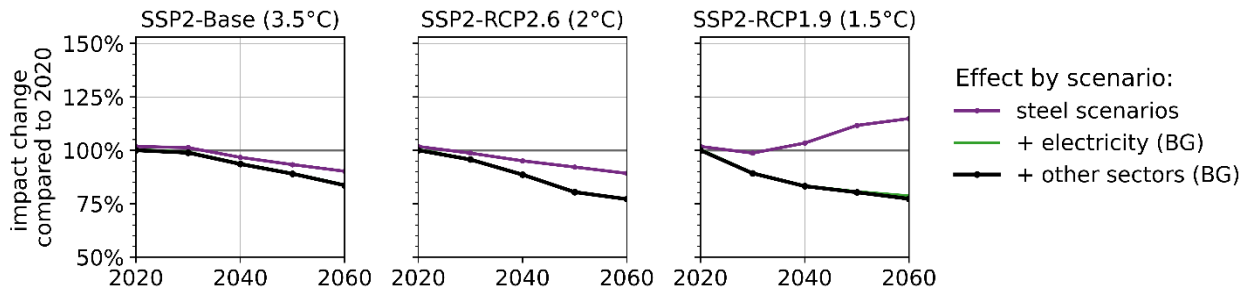
Acidification



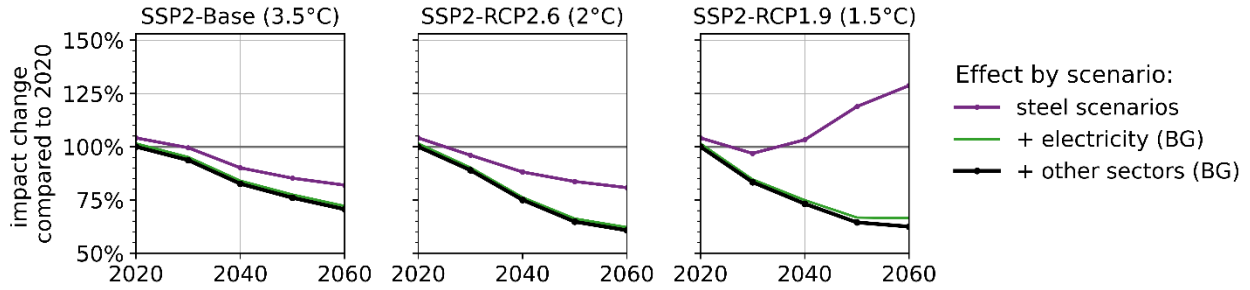
Climate Change (using IPCC, 2021, incl. biogenic C & H)



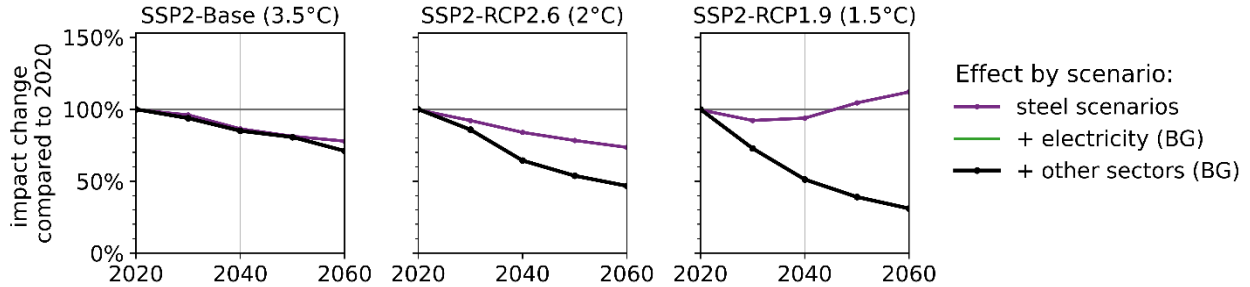
Ecotoxicity



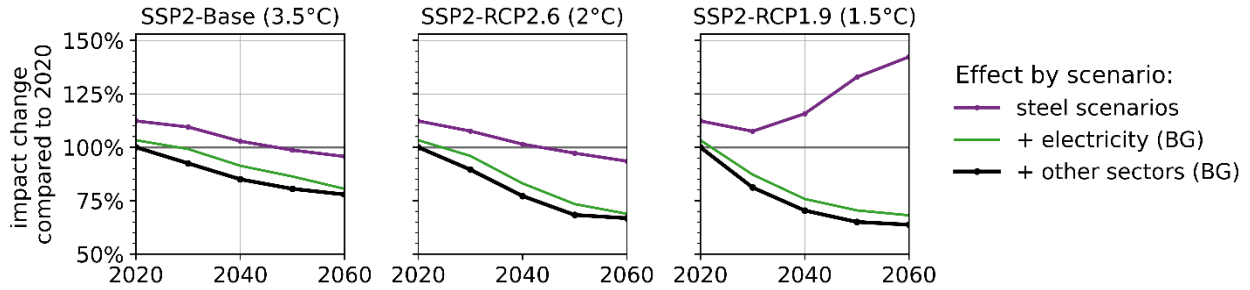
Energy resources, non-renew.



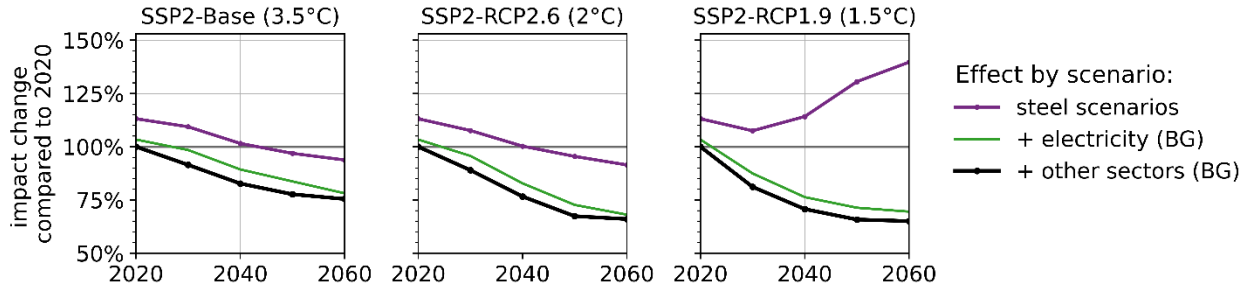
Eutrophication, freshwater



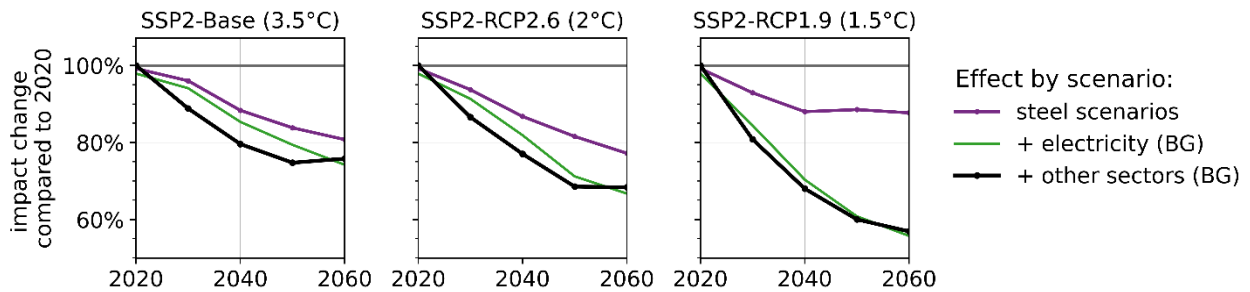
Eutrophication, marine



Eutrophication, terrestrial



Particulate matter



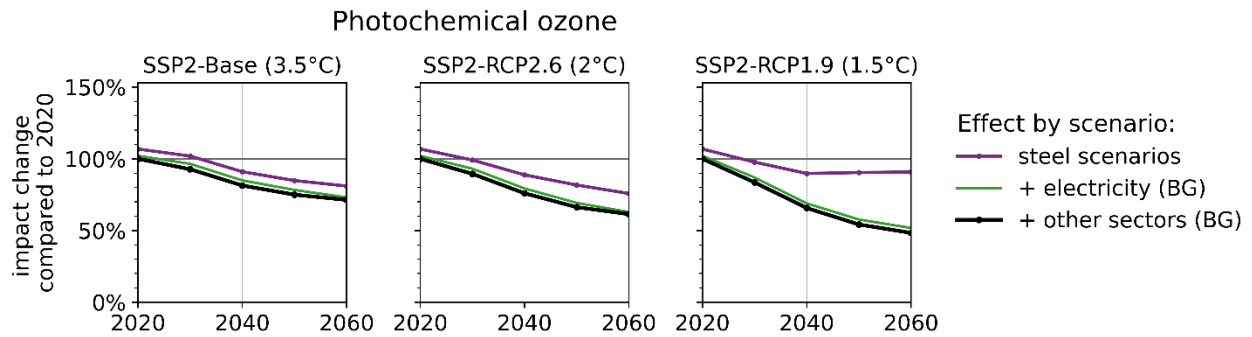


Figure S22: Impact developments for 1 kg of steel production for the global steel market from 2020 to 2060. Values are relative to the impacts in 2020 and the case where all background scenarios are incorporated (black line). The lines represent the impact change depending on which scenarios are implemented. Purple line: only steel scenarios; green line: steel + electricity scenarios; black line: all scenarios are implemented. The black line corresponds to the results presented in the main paper.

2.5. Normalization and weighting results

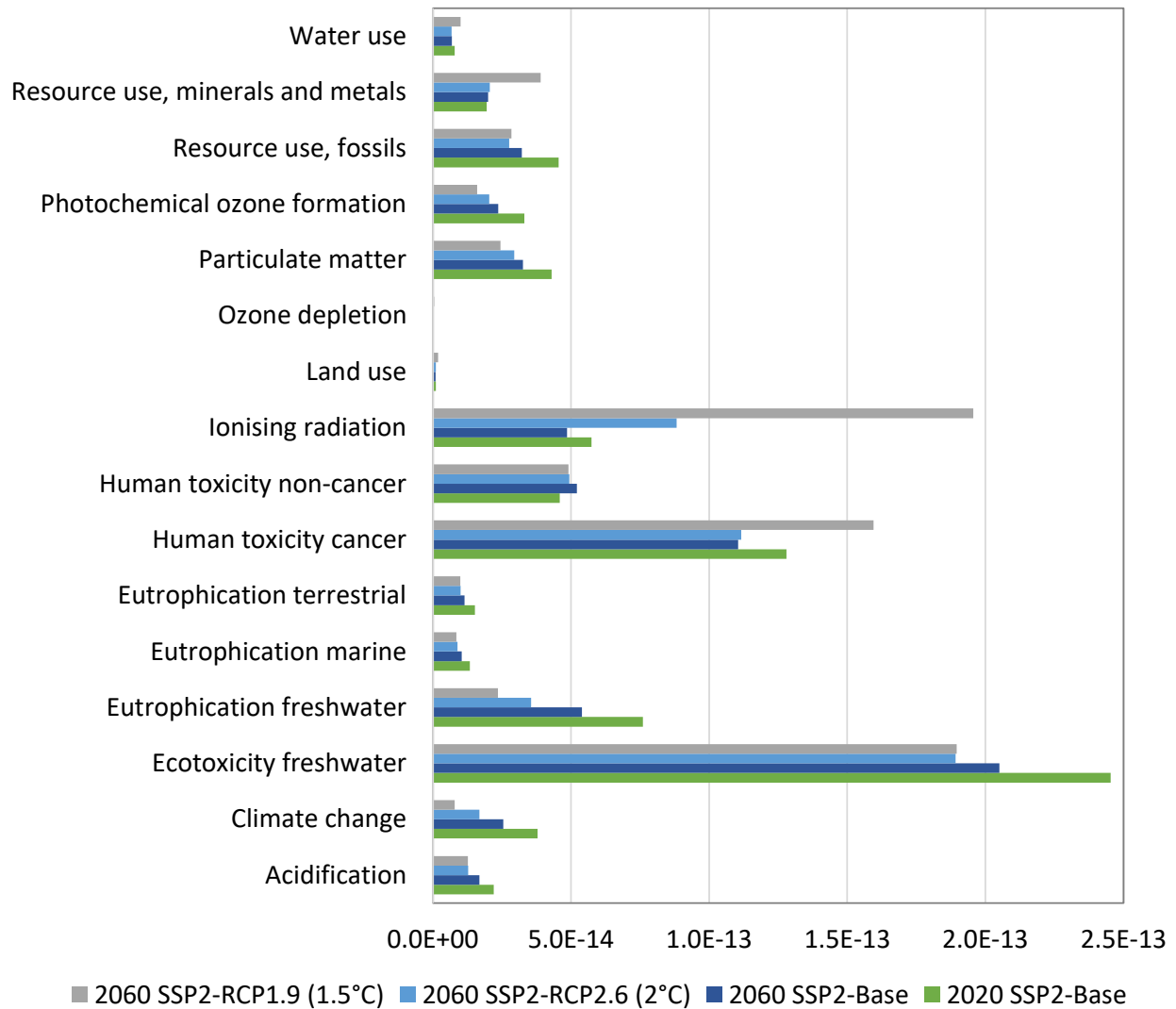
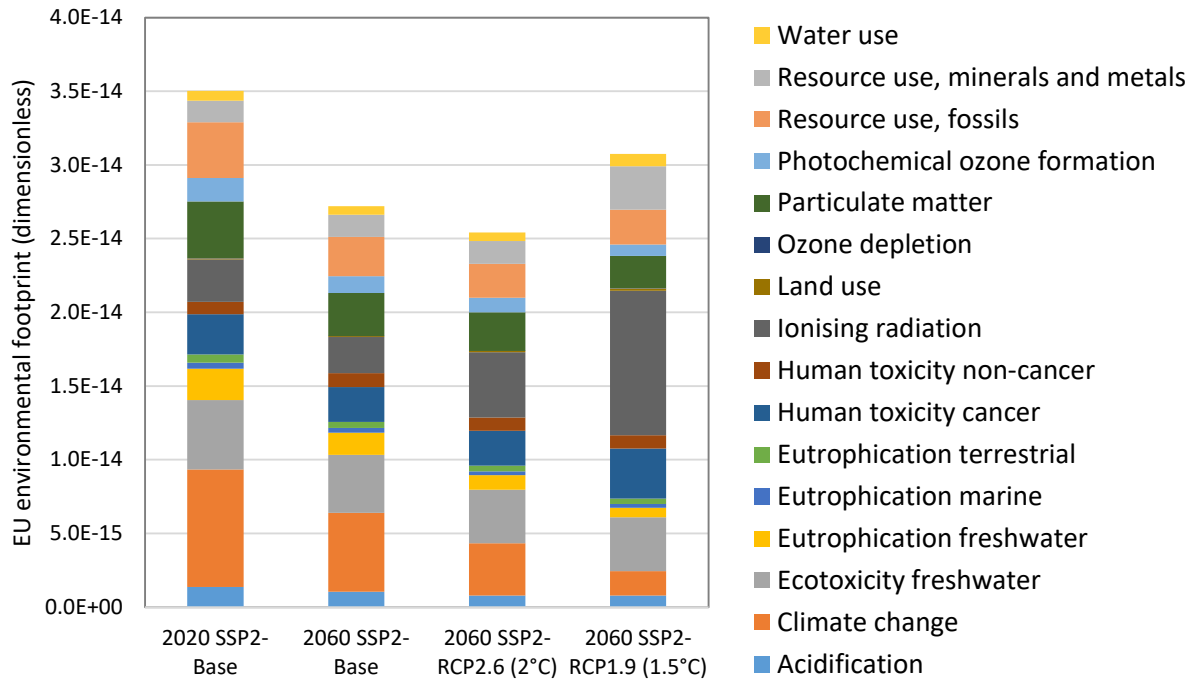


Figure S23: Normalized results calculated with global normalization factors for EF 3.0 from Crenna et al. (2019)⁴³. Functional unit: 1 kilogram of steel from the global market group for steel; premise: all background scenarios are incorporated.

a) EU Environmental footprint per kilogram of steel



b) EU Environmental footprint for global steel demand

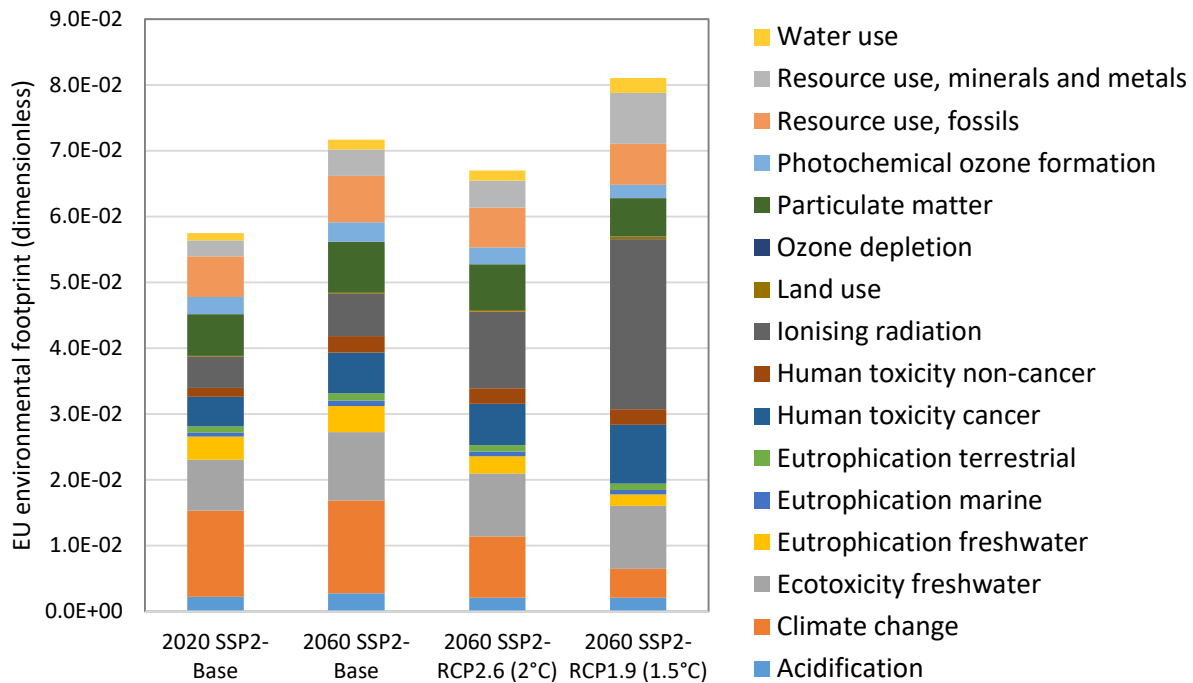


Figure S24: Weighted results using the EU Environmental footprint method (sources for weighting factors: Andreasi Bassi et al. (2023)⁴⁴, which is based on Sala et al. (2018)⁴⁵). Functional units: a) 1 kilogram of steel from the global market group for steel, b) global steel production via the global market group for steel; premise: all background scenarios are incorporated.

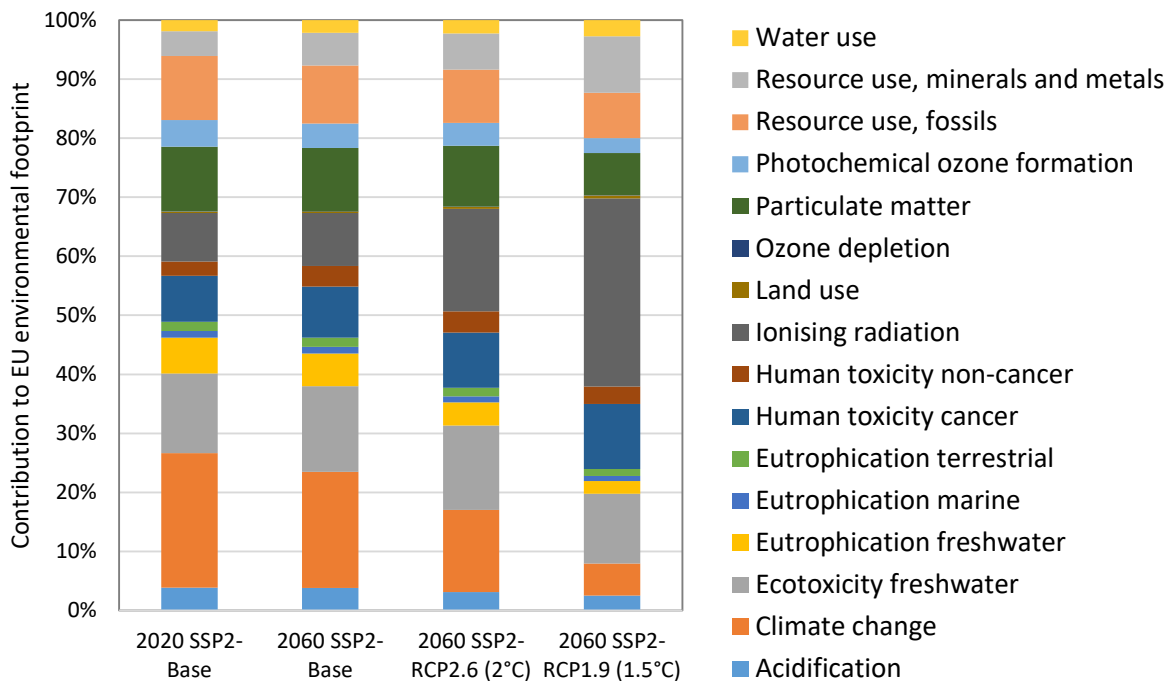


Figure S25: Relative shares for the weighted results shown in Figure S24.

If the impacts of global steel production are calculated using the EU environmental footprint (EF) method, it becomes apparent that climate change will not be the largest contributor in the future. It is the major driver of the current impacts (in 2020, its share is 23%), but in a decarbonized steel supply it becomes less prominent compared to other impact categories, contributing 14% or 5% in the 2°C and 1.5°C scenario respectively, by 2060 (Figure S25).

By 2060, the total EF is higher in the 1.5°C scenario than in the Base scenario and 2°C scenario per kg of steel produced, mainly due to rising impacts in ionising radiation (Figure S24.a). Ionising radiation (IR) is caused by nuclear power, specifically slag treatment from uranium milling, which is needed to satisfy the high electricity demand for an electrified steel production. IR impacts could be lowered in the future through improved slag treatment. However, it is unknown to what extent this can further reduce IR impacts.

Considering rising steel demand (Figure S24.b), the EF of future global steel production will increase by 2060 compared to 2020 for all scenarios. The 1.5°C scenario exhibits the highest increase of 41% by 2060, while the EF of the Base and 2°C scenario increase to a lesser extent, i.e., by 25% and 17% respectively. This increase is not driven by climate change, which overall has a declining impact, but by the other categories (e.g., IR, metal depletion, carcinogenic human toxicity, and to some extent, freshwater ecotoxicity).

Overall, these results indicate that climate change impacts are not the sole concern of steel production. However, they should be interpreted within the bounds of methodological constraints and assumptions inherent to the EU EF approach⁴⁶. Schenker et al. (2022)³⁸ demonstrate a similar finding using Recipe endpoint indicators for the future impacts of steel production. Likewise, they show that climate change is likely to play a minor role compared to, e.g., toxicity impacts.

Despite the uncertainty of future impact prevention measures and the limitation of the EF method, these results show that in the future, more impact categories than climate change may be relevant to maintain ecosystem quality and reduce the health impacts of humans living near industrial sites.

Climate change might be the most pressing issue today, also due to its effects on a global scale. However, other impact categories can have direct (and indirect) effects on the local environments and people. For

example, water use might not be the primary concern of steel production at the global level compared to other sectors like agriculture. However, mining and processing activities for metal production can still be relevant and an issue in regions of water scarcity, as highlighted by Northey et al. (2016)⁴⁷ and Schenker et al. (2022)³⁸. Another example is deforestation and biodiversity loss being driven by iron and the needed coal mining, .e.g., in Brazil^{48,49}, although iron mining may not be the main driver of these impacts at the global level.

Furthermore, Schenker et al. (2022)³⁸ and Watari et al. (2021)⁵⁰ stress that impact categories other than climate change are relevant for metal production, such as water use, chemical pollution or biodiversity loss. However, planetary boundaries have not been determined yet for all impact categories, e.g. for chemical pollution³⁸.

Approaches applying various methods, including local and global perspectives, are required to assess and understand the diverse impacts of a complex supply chain. These could include planetary boundaries and assessments of local impacts, e.g., via regionalised LCA, to avoid problem-shifting to specific regions. Although such additional assessments are beyond the scope of this study, our work and LCI data can serve as a basis for future research.

3 Discussion

3.1. Explorative scenario with a shift to green H2-DRI

Scenario description and assumptions

For exploration purposes, we examined a scenario with high shares of green H2-DRI, as shown in Figure S26. This is based on the following assumptions:

- It is derived from the scenario SSP2-RCP1.9 (1.5°C) with BF-BOF, NG-DRI and scrap-EAF producing the identical amounts as in SSP2-RCP1.9. Thus, the phase-out of BF-BOF is the same.
- No new capacities are built for technologies with insufficient emission reduction potential, including CCS technologies.
- Existing capacities for TGR-BF-BOF in 2020 are phased out by 2040, assuming a remaining lifetime of 20 years.
- EW is not introduced, representing the case where it does not reach market maturity soon enough.
- Thus, primary production shifts to green H2-DRI as the main production route to replace BF-BOFs and will produce 61% by 2060. It furthermore replaces the average H2-DRI, which sources hydrogen from the average hydrogen market.

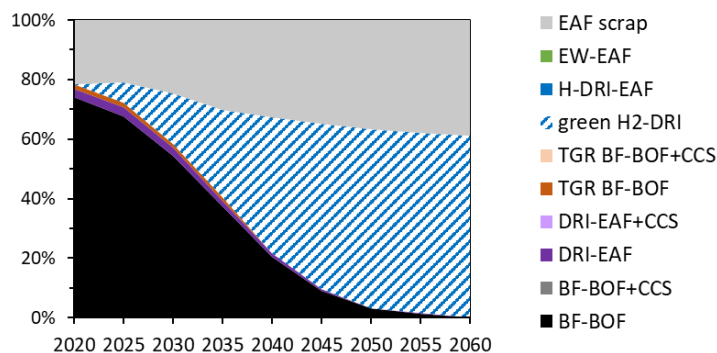


Figure S26: Production mix of global steel production as an explorative scenario with green H2-DRI-EAF.

Resulting GHG emissions

To calculate the emission reduction potential of this scenario, we applied a simplified model based on the following assumptions:

- Emission intensities are based on world datasets for each production route for unalloyed steel production with all background scenarios integrated.
- The entire steel demand is fulfilled by unalloyed steel, using world datasets for each production technology. This assumption applies to both the green H2-DRI scenario, but also to create a simplified SSP2-RCP1.9 scenario.
- The emission reduction potential is the difference between the cumulative emissions of the simplified SSP2-RCP1.9 steel scenario and the simplified green H2-DRI steel scenario by 2060.

The simplified green H2-DRI scenario reduces cumulative GHG emissions by -16% compared to the simplified SSP2-RCP1.9 scenario by 2060.

Limitations

Please note that this scenario constitutes an explorative scenario, which is not generated by IMAGE but created and assessed with simplified assumptions as described in the previous sections. This scenario thus complements the three scenarios from IMAGE, which do not foresee a shift to green H2-DRI despite current industrial trends.

IMAGE provides cost-optimal decarbonization pathways for various sectors, including energy, steel and hydrogen supply, considering the emission constraints of different climate mitigation targets. For H2-DRI, it assumes that hydrogen is sourced from the average region-specific hydrogen market. If the resulting scenarios from IMAGE do not anticipate a large share of H2-DRI, this implies that other technologies perform better than H2-DRI under the constraints of costs and emission intensities.

The main goal of this additional explorative scenario is to account for current trends towards green H2-DRI and to estimate the maximum emission reduction potential of an ambitious transition to green H2-DRI.

Due to its simplified assumptions, this explorative scenario is subject to certain limitations. For example, the energy and steel scenarios are not internally coherent since IMAGE did not generate this steel scenario. Hence, the assumption that green hydrogen is solely produced from wind power does not reflect potential technological and regional variations, as they usually occur in dynamic energy systems. Our assumption for green hydrogen represents an optimal scenario that aims to determine the lower boundary of future GHG emissions, considering the best case for green H2-DRI.

3.2. Limitations

This chapter provides additional limitations which can serve as a basis to improve the LCIs and scenario assessments in future studies.

3.2.1. Scenarios from IMAGE

Like any model, IAMs have certain limitations, and the scenarios are to be interpreted in the context of the respective modelling characteristics. This means the scenarios are rather exploratory, i.e., *what-if* scenarios, than predictions. As any scenario, they are subject to uncertainties—a challenge that applies not only to the IAM or IMAGE community but also to the general research field of future studies. As such, the scenarios provide insights into *directions* of future developments under specific rule-sets, constraints, and general global societal developments. However, the results should not be interpreted as *absolute* values but rather used to gain insights about the consequences of potential future developments.

Furthermore, IMAGE is a process-based IAM that strongly focuses on physical flows and relationships, while economic IAMs prioritize cost analyses⁵¹. As such, IMAGE is less suited for economic evaluations. However, future research could leverage the strength of both approaches by linking IMAGE with an economic IAM to enable an assessment of economic drivers and implications of industrial decarbonization pathways.

Representation of the steel sector:

There is a lack of data in the steel scenarios from IMAGE for:

- Production amounts and pathways per steel type, such as low-alloyed, reinforcing or chromium steel. Thus, the regional production shares from IMAGE are assumed for all steel types. Furthermore, the production share of steel types is assumed to be constant based on data from ecoinvent.
 - o Future research could include the demand by type to improve the accuracy of impacts and the effects of new grades, e.g. for more light-weight transport and machinery. For example, scenarios for chromium steel production could be very valuable, as chromium steel has a considerably higher impact than the other steel types.
 - o Moreover, the suitability of novel production routes for each steel type is currently not considered in detail, as the demand per steel type is lacking. This could be improved when demand scenarios for each steel type exist. For example, scrap-based production may not be suitable for all steel types, such as high-end steel types, depending on scrap composition and contamination.
- Efficiency improvements per sub-process within a steel production route, like pellet and sinter production or hot rolling, may have varying efficiency improvements. Therefore, we applied the efficiency improvements to the main iron and steel production processes for each route, such as, BF, BOF, DRI or EAF (see Figure S12).

Distinction between primary and secondary steel production:

As described in section 1.4.5, primary and secondary production routes are assumed to be separated systems, where scrap-EAFs are purely operated using scrap, and primary production is purely based on primary iron-bearing material. This simplification does not fully reflect industrial practices, where input streams tend to be a mix of primary and secondary materials. For instance, scrap is to some degree fed into primary production routes, e.g., BOFs by up to 30%³⁹, while scrap-EAFs tend to blend pig iron or DRI with scrap for quality control and process stability.

Our model assumes separated production routes based on a modular approach for the following reasons:

- The blending of primary and secondary material is highly variable. It is decided on a plant-by-plant basis depending on multiple factors, such as material availability and quality, contamination, material and energy prices, or desired output material of a specific steel type. These factors are highly dynamic, region- and even plant-specific. As such, they are very difficult to project at this level of detail. There is a lack of required data per region with global coverage, even for current practices.
- Incorporating an additional parameter for variable mixes of scrap and iron per production route and region is currently out of the scope of the IMAGE model.

- This separation is necessary to correctly account for the scrap availability, which is determined by the IMAGE scenarios based on an endogenous material stock model.
- While we acknowledge that this is a simplification, it enables a fair comparison of the different production routes under clear boundary conditions and supports scenario clarity.
- Furthermore, the lack of mixed input streams balances itself out to some degree, as the inputs of primary and secondary material in the other route and their consequences on increasing versus lowering impacts partly offset each other. Therefore, this simplification might be relatively benign overall, and its final effect is considered within the range of uncertainty of the scenario results.

Incorporating the parameter of mixed input streams implies various challenges, especially related to the clarity and interpretability of the results, as it:

- adds another factor of very high uncertainty;
- hinders a fair comparison across production routes and regions;
- this might lead to underestimating primary production and overestimating secondary production impacts, which is the less preferred option compared to the current case, where our simplification might lead to overestimating primary production impacts and underestimating secondary production impacts. Underestimating primary production and overestimating secondary production impacts could distort the results and thus have harmful consequences for policy recommendations.

We therefore recommend this aspect as a direction for further research.

Energy scenarios:

The electricity scenarios are a key driver of the future environmental impacts of steel production, if steel production will undergo an electrification as assumed in our 1.5°C scenario, as this will considerably increase future electricity requirements.

On a per-kg-steel basis, impacts are expected to increase in ionising radiation, land use, material resources, and potentially ozone depletion and human toxicity under the 1.5°C scenario, as shown in Figure 8. Similarly, impacts in ionising radiation, land use, material resources, and ozone depletion are likely to increase per kWh of electricity generated under the 1.5°C scenario from IMAGE (see section 2.2.2), suggesting a correlation. Furthermore, the influence of the BG electricity scenario compared to considering the steel scenarios alone is illustrated in section 2.4.

The IMAGE scenarios for electricity are optimized for reducing climate change emissions. To considerably reduce GHG emissions of electricity generation, IMAGE assumes drastic capacity extensions for nuclear power and CCS-based power generation (see section 1.2.5). However, these are the primary causes of rising impacts in ionising radiation and land use (see section 3.3.1 in the paper).

Further research is needed to explore options to avoid the potential burden-shifting of the decarbonization measures to the aforementioned categories. This could include improving the data quality of the driving processes (e.g., uranium mining) and identifying respective emission mitigation technologies. More importantly, alternative electricity scenarios should be considered. While IMAGE relies on nuclear power and CCS-based power generation, other IAMs pursue other strategies, such as REMIND, which instead foresees a significant shift to renewables⁵².

This research aimed at assessing internally consistent energy and steel scenarios of global coverage while accounting for a shift to novel steel production technologies. At the time of writing, these existed only from

the IAM IMAGE, as REMIND lacked sufficient technological resolution for the steel sector. If such suitable scenarios become available, further insights into future steel and energy supply could be gained from alternative scenarios generated by other models, such as REMIND. For this, the LCIs and Python code provided by this study could form a starting point.

3.2.2. Premise

- The production volumes of the IMAGE scenarios specify the sum of domestic production and production for export. However, they do not provide a complete and consistent trade balance, neither for iron and steel nor for intermediate products, such as iron ore, iron ore pellets, pig iron, H₂-based sponge iron⁵³, different steel types, etc. Therefore, we assume that the supply chains take place in the respective IMAGE regions for the processes within our system boundary of steel production (Figure 2).
- The transport distances and types (e.g., road, train, or sea transport) in the regional markets are assumed to be the same as those in the existing market datasets in ecoinvent and are thus not region-specific.
- The background scenarios for future heat supply could be further improved. Heat supply can play an important role, especially in industrial high-temperature processes. While the heat scenarios in this study consider future fuel mixes for heat supply, e.g., synthetic gas, biogas or natural gas for gas boilers, they do not account for future technology mixes, i.e. transitions in technological choices providing the heat.

3.2.3. LCIs of steel production processes

BF-BOF-CCS:

- The regeneration of monoethanolamine (MEA) requires steam. Literature states that steam is usually generated from natural gas^{6,34,54}. Technically, steam could also be generated from electric boilers, a mature technology. For MEA-CCS, saturated steam at 9 bar and 175°C would be required⁶, possibly with electric boilers⁵⁵. Yet, electric boilers are unlikely in the iron and steel industry, since the by-products from the iron and steel process are gases which can be directly used in combustion-based boilers, potentially supplemented with natural gas⁵⁵. Thus, electric boilers in the steel industry might face economic challenges. This aligns with the case study we used as the data source for our LCIs⁶, where the additional natural gas represents 13.6% of thermal input to the steam generation plant, while the remaining 84.4% are supplied by BF and BOF gases. Hence, we assume natural gas as fuel for additional steam demand.
 - o Future research is needed to determine how such auxiliary processes in industry can be further electrified.
- For the additional energy required for the MEA-CCS process, we assumed additional natural gas requirements of 2.71 MJ natural gas/kg CO₂ based on a case study for a respective steel production plant⁶. Although this is aligned with the assumptions in IMAGE and previous research^{54,56}, it can be considered somewhat on the lower end according to a recent literature review⁵⁷, which identified a thermal energy requirement of 1.3 - 6.2 MJ/kg CO₂. However, our results show that even under our rather optimistic assumptions for the BF-BOF-CCS production route, this technology is outperformed by (indirectly) electrified technologies, like H₂-DRI and EW, regarding GHG emission intensity.

TGR-BF-BOF:

- Hydrogen (H₂) emissions may also be reduced, as H₂ in the top gas may be recycled^{7,8,19}. We could not account for this reduction due to a lack of data for the H₂ emissions and reduction rate in (TGR-) BFs.
- The literature does not provide data about the consequences of top gas recycling for other emissions (apart from CO₂, CO, NO_x, SO₂, and particulate matter). Hence, this study does not account for them.

TGR-BF-BOF, TGR-BF-BOF+CCS, NG-DRI+CCS:

- Due to a lack of data, the dust removal rate in the gas pre-treatment was assumed to be for CCS using MEA.
- Due to a lack of data, cryogenic CO₂ separation and compression is modelled solely using electricity and CO₂ requirements.
- The zeolite production process in ecoinvent contains an aggregated inventory: it has no inputs from other processes and only aggregated environmental emissions.

H2-DRI:

- Hydrogen production is a major driver of future impacts of H₂-DRI. To ensure consistency with the IMAGE scenarios across sectors, we assume that the hydrogen used for H₂-DRI is sourced from the regional hydrogen market mix.
 - o Future research could investigate optimal hydrogen production conditions to minimize the environmental impact of H₂-DRI.

EW:

- The requirements and the source of electrolyte (sodium hydroxide) for iron production via EW are uncertain. In this study, we assume an amount of 1.5 kg / kg iron oxide (Fe₂O₃)¹² and a recycling rate of 50%⁵⁸, leading to a makeup amount of 0.75 kg / kg Fe₂O₃. Moreover, we assume that sodium hydroxide is sourced from the global market dataset available in ecoinvent, which uses various production technologies (chlor-alkali electrolysis, diaphragm cell, membrane cell, mercury cell). The electrolyte input has proven to be a main contributor to impacts of iron from EW⁵⁹ due to the highly energy-intensive production of sodium hydroxide. However, the environmental performance of sodium hydroxide production technologies can vary.
 - o To reduce the uncertainty of environmental impacts of EW, further insights into the requirements and low-emissions production options of sodium hydroxide are needed.

EAF:

- Literature provides LCIs for EAFs for different technologies, such as EW, H₂-DRI, and NG-DRI. These LCIs are at very different levels of detail both for material and energy requirements but also in terms of emissions. Using these LCIs from different sources would thus lead to inconsistencies and incomparable results among the production routes. Therefore, we used one data source for the EAF for all steel production routes requiring steelmaking via the EAF, i.e., a dataset from ecoinvent. The dataset of ecoinvent was the most comprehensive one. This dataset was adapted for primary and secondary production in a consistent way across production routes, as explained in sections 1.3 and

1.4.5. The focus of this study is the future environmental impacts of primary steel production. For primary steel production, the process of iron production is the most energy- and emission-intensive.

- Future research could address the influence of the type of iron-bearing input into EAFs.

Alloying elements:

- We modelled the alloying elements for low-alloyed and unalloyed steel based on data from existing ecoinvent processes. However, this could be done in greater detail. Alloying elements can influence impacts considerably, e.g., for climate change by more than 15%.

4 References

- 1 E. Stehfest, D. van Vuuren, T. Kram, L. Bouwman, R. Alkemade, M. Bakkenes, H. Biemans, A. Bouwman, M. den Elzen, J. Janse, P. Lucas, J. van Minnen, M. Müller and A. Prins, *Integrated Assessment of Global Environmental Change with IMAGE 3.0. Model description and policy applications*, The Hague, 2014.
- 2 M. A. van Sluiseveld, H. S. de Boer, V. Daioglou, A. F. Hof and D. P. van Vuuren, A race to zero - Assessing the position of heavy industry in a global net-zero CO2 emissions context, *Energy and Climate Change*, 2021, **2**, 100051.
- 3 B. J. van Ruijven, D. P. van Vuuren, W. Boskaljon, M. L. Neelis, D. Saygin and M. K. Patel, Long-term model-based projections of energy use and CO2 emissions from the global steel and cement industries, *Resources, Conservation and Recycling*, 2016, **112**, 15–36.
- 4 M. Arens, E. Worrell, W. Eichhammer, A. Hasanbeigi and Q. Zhang, Pathways to a low-carbon iron and steel industry in the medium-term – the case of Germany, *Journal of Cleaner Production*, 2017, **163**, 84–98.
- 5 E. Worrell, L. Price, M. Neelis, C. Galitsky and N. Zhou, World best practice energy intensity values for selected industrial sectors, 2007.
- 6 IEAGHG, Iron and Steel CCS Study (Techno-economics Integrated Steel Mill). Report 2013/04, 2013.
- 7 A. Keys, M. van Hout and B. Daniëls, *Decarbonisation options for the Dutch Steel Industry*, PBL Netherlands Environmental Assessment Agency & ECN part of TNO, The Hague, 2019, https://www.pbl.nl/sites/default/files/downloads/pbl-2019-decarbonisation-options-for-the-dutch-steel-industry_3723.pdf.
- 8 M. A. Quader, S. Ahmed, S. Z. Dawal and Y. Nukman, Present needs, recent progress and future trends of energy-efficient Ultra-Low Carbon Dioxide (CO) Steelmaking (ULCOS) program, *Renewable and Sustainable Energy Reviews*, 2016, **55**, 537–549.
- 9 M. Shahabuddin, G. Brooks and M. A. Rhamdhani, Decarbonisation and hydrogen integration of steel industries: Recent development, challenges and technoeconomic analysis, *Journal of Cleaner Production*, 2023, **395**, 136391.
- 10 T. Kuramochi, A. Ramírez, W. Turkenburg and A. Faaij, Comparative assessment of CO2 capture technologies for carbon-intensive industrial processes, *Progress in Energy and Combustion Science*, 2012, **38**, 87–112.
- 11 V. Vogl, M. Åhman and L. J. Nilsson, Assessment of hydrogen direct reduction for fossil-free steelmaking, *Journal of Cleaner Production*, 2018, **203**, 736–745.
- 12 EC, *Iron production by electrochemical reduction of its oxide for high CO2 mitigation. IERO final report*, Brussels, 2016, <https://op.europa.eu/en/publication-detail/-/publication/4255cd56-9a96-11e6-9bca-01aa75ed71a1>.
- 13 IMAGE,

Region	classification	map,
--------	----------------	------

https://models.pbl.nl/index.php?title=Region_classification_map&oldid=3324, (accessed 13 August 2024UTC).

- 14 B. van Ruijven, D. P. van Vuuren and B. de Vries, The potential role of hydrogen in energy systems with and without climate policy, *International Journal of Hydrogen Energy*, 2007, **32**, 1655–1672.
- 15 B. van Ruijven, F. Urban, R. M. Benders, H. C. Moll, J. P. van der Sluijs, B. de Vries and D. P. van Vuuren, Modeling Energy and Development: An Evaluation of Models and Concepts, *World Development*, 2008, **36**, 2801–2821.
- 16 E. van der Voet, L. van Oers, M. Verboon and K. Kuipers, Environmental Implications of Future Demand Scenarios for Metals: Methodology and Application to the Case of Seven Major Metals, *Journal of Industrial Ecology*, 2019, **23**, 141–155.
- 17 C. Harpprecht, L. van Oers, S. A. Northey, Y. Yang and B. Steubing, Environmental impacts of key metals' supply and low-carbon technologies are likely to decrease in the future, *Journal of Industrial Ecology*, 2021. DOI: 10.1111/jiec.13181.
- 18 C. Harpprecht, R. Sacchi, T. Naegler, M. van Sluisveld, V. Daioglou, A. Tukker and B. Steubing, *Code and data for publication: Future Environmental Impacts of Global Iron and Steel Production. v1.0.0*, 2025, <https://doi.org/10.5281/zenodo.14968094>.
- 19 H.-D. Choi, *Hybrid life cycle assessment of steel production with carbon capture and storage*. Master Thesis, NTNU, Trondheim, 2013, <https://ntnuopen.ntnu.no/ntnu-xmlui/handle/11250/235312>.
- 20 A. Otto, M. Robinius, T. Grube, S. Schiebahn, A. Praktijnjo and D. Stolten, Power-to-Steel: Reducing CO₂ through the Integration of Renewable Energy and Hydrogen into the German Steel Industry, *Energies*, 2017, **10**. DOI: 10.3390/en10040451.
- 21 A. Hasanbeigi, M. Arens and L. Price, Alternative emerging ironmaking technologies for energy-efficiency and carbon dioxide emissions reduction: A technical review, *Renewable and Sustainable Energy Reviews*, 2014, **33**, 645–658.
- 22 E. I. Nduagu, D. Yadav, N. Bhardwaj, S. Elango, T. Biswas, R. Banerjee and S. Rajagopalan, Comparative life cycle assessment of natural gas and coal-based directly reduced iron (DRI) production: A case study for India, *Journal of Cleaner Production*, 2022, **347**, 131196.
- 23 F. Li, M. Chu, J. Tang, Z. Liu, J. Guo, R. Yan and P. Liu, Thermodynamic performance analysis and environmental impact assessment of an integrated system for hydrogen generation and steelmaking, *Energy*, 2022, **241**, 122922.
- 24 M. Hölling and S. Gellert, Direct Reduction: Transition from Natural Gas to Hydrogen?, 2018.
- 25 A. Bhaskar, M. Assadi and H. Nikpey Somehsaraei, Decarbonization of the Iron and Steel Industry with Direct Reduction of Iron Ore with Green Hydrogen, *Energies*, 2020, **13**. DOI: 10.3390/en13030758.
- 26 Siderwin, *D7.4. Environmental life cycle assessment intermediary report*, 2020, <https://www.siderwin-spire.eu/sites/siderwin.drupal.pulsartecnalialia.com/files/documents/D7.4.Environmental%20life%20cycle%20assessment%20intermediary%20report.pdf>.
- 27 European Commission, ULCOS top gas recycling blast furnace process (ULCOS TGRBF). Research fund for coal and steel (EC), EUR, 26414., 2014. DOI: 10.2777/59481.
- 28 H. Lavelaine, SIDERWIN project: electrification of primary steel production for direct CO₂ emission avoidance, *METEC*, 2019, 2019.
- 29 G. Zhao, M. R. Kraglund, H. L. Frandsen, A. C. Wulff, S. H. Jensen, M. Chen and C. R. Graves, Life cycle assessment of H₂O electrolysis technologies, *International Journal of Hydrogen Energy*, 2020, **45**, 23765–23781.
- 30 Siderwin, *SIDERWIN webinar. SIDERWIN: A breakthrough technology to decarbonize primary steel production through direct electrification*, 2021.
- 31 C. Wulf and M. Kaltschmitt, Hydrogen Supply Chains for Mobility—Environmental and Economic Assessment, 2018, **10**, 1699.
- 32 A. Müller, C. Harpprecht, R. Sacchi, B. Maes, M. van Sluisveld, V. Daioglou, B. Šavija and B. Steubing, Decarbonizing the cement industry: Findings from coupling prospective life cycle assessment of clinker with integrated assessment model scenarios, *Journal of Cleaner Production*, 2024, **450**, 141884.
- 33 B. Singh, A. H. Strømman and E. G. Hertwich, Comparative life cycle environmental assessment of CCS technologies, *International Journal of Greenhouse Gas Control*, 2011, **5**, 911–921.

- 34 M. Voldsund, S. Gardarsdottir, E. de Lena, J.-F. Pérez-Calvo, A. Jamali, D. Berstad, C. Fu, M. Romano, S. Roussanaly, R. Anantharaman, H. Hoppe, D. Sutter, M. Mazzotti, M. Gazzani, G. Cinti and K. Jordal, Comparison of Technologies for CO₂ Capture from Cement Production—Part 1: Technical Evaluation, *Energies*, 2019, **12**. DOI: 10.3390/en12030559.
- 35 K. Volkart, C. Bauer and C. Boulet, Life cycle assessment of carbon capture and storage in power generation and industry in Europe, *International Journal of Greenhouse Gas Control*, 2013, **16**, 91–106.
- 36 UK steel, *Briefing: The UK steel industry and the green transition*, UK steel, 2024, https://www.uksteel.org/versions/2/wizard/modules/fileManager/downloadDigitalFile.php?url=https%3A%2F%2Fstatic.s123-cdn-static-d.com%2Fuploads%2F8346772%2Fnormal_65b29308edd87.pdf, (accessed 5 February 2025).
- 37 M. Sand, R. B. Skeie, M. Sandstad, S. Krishnan, G. Myhre, H. Bryant, R. Derwent, D. Hauglustaine, F. Paulot, M. Prather and D. Stevenson, A multi-model assessment of the Global Warming Potential of hydrogen, *Commun Earth Environ*, 2023, **4**. DOI: 10.1038/s43247-023-00857-8.
- 38 V. Schenker, V. Kulionis, C. Oberschelp and S. Pfister, Metals for low-carbon technologies: Environmental impacts and relation to planetary boundaries, *Journal of Cleaner Production*, 2022, **372**, 133620.
- 39 R. Remus, M. A. Aguado-Monsonet, S. Roudier and L. D. Sancho, *Best Available Techniques (BAT) reference document for iron and steel production: Industrial emissions directive 2010/75/EU: integrated pollution prevention and control (No. JRC69967)*, Joint Research Centre (Seville), 2013.
- 40 G. Doka, *Life Cycle Inventories of Waste Treatment Services. ecoinvent report. No. 13. Swiss Centre for Life Cycle Inventories, Dübendorf*, 2003.
- 41 UNEP, *Country data. Consumption of controlled substances. Accessed 19 May 2025*, 2024, <https://ozone.unep.org/countries/data>.
- 42 A. E. van den Oever, S. Puricelli, D. Costa, N. Thonemann, M. Lavigne Philippot and M. Messagie, Revisiting the challenges of ozone depletion in life cycle assessment, *Cleaner Environmental Systems*, 2024, **13**, 100196.
- 43 E. Crenna, M. Secchi, L. Benini and S. Sala, Global environmental impacts: data sources and methodological choices for calculating normalization factors for LCA, *Int J Life Cycle Assess*, 2019, **24**, 1851–1877.
- 44 S. Andreasi Bassi, F. Biganzoli, N. Ferrara, A. Amadei, A. Valente and S. Sala, *Updated characterisation and normalisation factors for the environmental footprint 3.1 method*, Europäische Kommission, JRC technical report JRC130796, Luxembourg, 2023, <https://op.europa.eu/en/publication-detail/-/publication/145f8401-a82a-11ed-b508-01aa75ed71a1>.
- 45 Sala S., Cerutti A.K., Pant R., *Development of a weighting approach for the environmental footprint*, European Commission EUR 28562, Luxembourg, 2018.
- 46 M. Pizzol, A. Laurent, S. Sala, B. Weidema, F. Verones and C. Koffler, Normalisation and weighting in life cycle assessment: quo vadis?, *Int J Life Cycle Assess*, 2017, **22**, 853–866.
- 47 S. A. Northey, G. M. Mudd, E. Saarivuori, H. Wessman-Jääskeläinen and N. Haque, Water footprinting and mining: Where are the limitations and opportunities?, *Journal of Cleaner Production*, 2016, **135**, 1098–1116.
- 48 L. J. Sonter, D. J. Barrett, C. J. Moran and B. S. Soares-Filho, Carbon emissions due to deforestation for the production of charcoal used in Brazil's steel industry, *Nat. Clim. Chang.*, 2015, **5**, 359–363.
- 49 L. J. Sonter, S. H. Ali and J. E. M. Watson, Mining and biodiversity: key issues and research needs in conservation science, *Proceedings. Biological sciences*, 2018, **285**. DOI: 10.1098/rspb.2018.1926.
- 50 T. Watari, K. Nansai and K. Nakajima, Major metals demand, supply, and environmental impacts to 2100: A critical review, *Resources, Conservation and Recycling*, 2021, **164**, 105107.
- 51 J. Weyant, Some Contributions of Integrated Assessment Models of Global Climate Change, *Review of Environmental Economics and Policy*, 2017, **11**, 115–137.
- 52 R. Sacchi, T. Terlouw, A. Dirnauchner, C. Bauer, B. Cox, C. Mutel, V. Daioglou and G. Luderer, PRospective EnvironMental Impact asSEment (premise): a streamlined approach to producing databases for

- prospective Life Cycle Assessment using Integrated Assessment Models, *Renewable and Sustainable Energy Reviews*, 2021. DOI: 10.1016/j.rser.2022.112311.
- 53 S. Bilici, G. Holtz, A. Jülich, R. König, Z. Li, H. Trollip, B. M. Call, A. Tönjes, S. S. Vishwanathan, O. Zelt, S. Lechtenböhmer, S. Kronshage and A. Meurer, Global trade of green iron as a game changer for a near-zero global steel industry? - A scenario-based assessment of regionalized impacts, *Energy and Climate Change*, 2024, **5**, 100161.
- 54 D.-A. Chisalita, L. Petrescu, P. Cobden, H. A. J. van Dijk, A.-M. Cormos and C.-C. Cormos, Assessing the environmental impact of an integrated steel mill with post-combustion CO₂ capture and storage using the LCA methodology, *Journal of Cleaner Production*, 2019, **211**, 1015–1025.
- 55 M. J. S. Zuberi, A. Hasanbeigi and W. Morrow, Electrification of industrial boilers in the USA: potentials, challenges, and policy implications, *Energy Efficiency*, 2022, **15**. DOI: 10.1007/s12053-022-10079-0.
- 56 C. Harpprecht, T. Naegler, B. Steubing, A. Tukker and S. Simon, Decarbonization scenarios for the iron and steel industry in context of a sectoral carbon budget: Germany as a case study, *Journal of Cleaner Production*, 2022, **380**, 134846.
- 57 J. Perpiñán, B. Peña, M. Bailera, V. Eveloy, P. Kannan, A. Raj, P. Lisbona and L. M. Romeo, Integration of carbon capture technologies in blast furnace based steel making: A comprehensive and systematic review, *Fuel*, 2023, **336**, 127074.
- 58 Siderwin, *SIDERWIN Concluding Webinar 2023. Webinar questions by participants*, 2023, https://www.siderwin-spire.eu/sites/siderwin.drupal.pulsartecnalia.com/files/documents/SIDERWIN_Webinar2023_QA_FINAL.pdf.
- 59 C. Harpprecht, T. Naegler, B. Steubing and R. Sacchi, *Prospective Life Cycle Assessment of the Electricity-Based Primary Steel Production Technology of Electrowinning.*, 2022, <https://elib.dlr.de/191406/>.